Major Project –II

"SOME STUDIES ON FRICTION STIR WELDING OF Al 6082 ALUMINIUM ALLOYS"

Submitted to **Delhi Technological University** in partial fulfillment of the requirement for the award of the Degree of

Master of Technology

In

PRODUCTION ENGINEERING

By

MOHD RASHID (2K13/PIE/11)

Under the supervision of

Mr. N.YUVRAJ

Assistant Professor

Mechanical Engineering Department

Delhi Technological University,

Shahabad Daulatpur

Bawana Road, Delhi-110042

Session 2013-2015

DECLARATION

I, hereby declare that the work embodied in the dissertation entitled "**SOME STUDIES ON FRICTION STIR WELDING OF Al 6082 ALUMINIUM ALLOYS**" in partial fulfillment for the award of degree of MASTER of TECHNOLOGY in "**PRODUCTION ENGINEERING**", is an original piece of work carried out by me under the supervision of Mr.N.Yuvraj (Assistant Professor), Mechanical Engineering Department, Delhi Technological University. The matter of this work either full or in part have not been submitted to any other institution or University for the award of any other Diploma or Degree or any other purpose what so ever.

MOHD RASHID

Roll No.: 2K13/PIE/11

CERTIFICATE

This is to certify that the work embodied in the dissertation entitled "**SOME STUDIES ON FRICTION STIR WELDING OF Al 6082 ALUMINIUM ALLOYS**" by **MOHD RASHID**, (Roll No.-**2K13/PIE/11**) in partial fulfillment of requirements for the award of Degree of Master of Technology in **PRODUCTION ENGINEERING**, is an authentic record of student's own work carried by him under my supervision.

This is also certified that this work has not been submitted to any other Institute or University for the award of any other diploma or degree.

(**Mr.N.Yuvraj)**

Assistant Professor

Mechanical Engineering Department

Delhi Technological University

Delhi- 110042

ACKNOWLEDGEMENT

It is a pleasure to acknowledge our gratitude to all the people involved, directly or indirectly in the completion of this project. I would like to thank my project guide Mr.N.Yuvraj who devoted valuable hours for this assignment and providing the motivational guidance during the entire preparation of this project, answering the number of technical queries despite his busy schedule. His valuable suggestions, constructive criticism and timely help proved extremely fruitful.

I am thankful to Mr. Tek Chand, Mr. Netram and other project staff Mechanical Engineering department for all assistance during execution of this project work. I am also thankful to my fellow friends specially Shailesh kumar singh, Ashish singh, Krishna pratap singh, Pawan kr. yadav, Bhupendra singh, Piyush yadav and Hariom pandey and colleagues who were always there to lend a helping hand in the hour of need.

MOHD RASHID

Roll No.: 2K13/PIE/11

Table of content

DECLARATION ii

CERTIFICATE iii

ACKNOWLEDGEMENT iv

Table of content v

List of Figure vi

List of table vii

Abstract ix

CHAPTER-1 1

Introduction 1

1.1 Material flow and mechanism of joining 4

1.2 Factors Affecting FSW 6

1.2.1 Tool Geometry 6

1.2.2 Welding Parameters 7

1.2.3 Joint Design 7

1.2.4 Tool Tilt and Plunge Depth 8

CHAPTER-2 10

Literature review 10

CHAPTER-3 24

Experiment -1 Optimization of tensile strength of friction stir welded AA6082 by Response surface methodology (RSM). 24

3.1 Introduction 24

3.2 Workpiece Material 24

3.3 Tool used 25

3.4 Experimental setup 26

3.5 Experimental procedure 27

3.6 Development of mathematical model 29

3.6.1 Response surface methodology 29

3.6.2 Model for Tensile strength 31

3.6.3 Checking adequacy of model 31

3.6.4 Model for Microhardness 33

3.6.5 Checking adequacy of model 33

3.7 Result and analysis 34

3.7.1 Tensile strength 34

3.7.2 Optimising parameters 35
3.7.3 Microhardness 40
3.7.4 Optimizing Parameters 42
CHAPTER-4 47
Experiment 2- Microstructural and mechanical behaviours of Nano-TiC-reinforced AA6082 FSW Joints at optimized parameters. 47
3.8 Introduction 47
3.9 Workpiece Material 48
3.10 Tool Used 48
3.11 Experimental setup 49
3.12 Experimental procedure 49
3.13 Testing 50
3.13.1 Tensile Test 50
3.13.2 Micro hardness Test 51
3.13.3 Microstructural analysis 51
3.13.4 SEM (scanning electron microscopy) 51
3.13.5 EDX (energy dispersive X-ray spectroscopy) 52
3.14 Result and discussion 52
Conclusions 58
References 59

List of Figure

Figure 1- Schematic diagram of FSW 2
Figure 2 - Plunge depth & Tilt angle 9
Figure 3 - Tools used for FSW of AA6082 26
Figure 4 -Friction stir welding machine 27
Figure 5 -Tool and work holding device 27
Figure 6-Standard tensile test specimen 28
Figure 7 -Tensile specimen (a) before test (b) after test 29
Figure 8-Normal probability plot of residuals for tensile strength 35
Figure 9- Actual vs predicted response of tensile strength 36
Figure 10-Tensile strength at const. D/d 37
Figure 11-Tensile strength at const. welding speed 37
Figure 12-Tensile strength at const. rotational speed 38
Figure 13-Contour of tensile strength at const. D/d 38
Figure 14-Contour of tensile strength at const. weling speed 39
Figure 15-Contour of tensile strength at const. rotational speed 39
Figure 16- Normal plots of residuals for microhardness 41
Figure 17-Predicted vs actual graph for microhardness 41
Figure 18-Microhardness at const. D/d 43
Figure 19-Microhardness at const.welding speed 43
Figure 20-Microhardness at const.rotational speed 44
Figure 21-Contour of microhardness at const. D/d 44
Figure 22-Contour of Microhardness at const.weling speed 45
Figure 23-Contour of Microhardness at const. rotational speed 45
Figure 24-Friction stir welded AA6082 plate 48
Figure 25-Square shape pin tool 48
Figure 26- Cross section of plate to be welded 49
Figure 27-Tensile test Machine 50
Figure 28- Tensile test specimen before and after the test 51
Figure 29-SEM setup 52
Figure 30 -Tensile strength of different specimen 53
Figure 31- Micro hardness value of different specimen 54
Figure 32-Micro structure of FSW AA 6082 -TiC alloy 55

Figure 33 SEM micro graph of FSW AA66082-TiC joint 56
Figure 34-SEM micrograph of fracture surface of FSW AA6082-TiC alloy 57
Figure 35-EDX analysis graph 57

List of table

Table 1 Chemical composition of AA6082-T651 24
Table 2 Tool specification 25
Table 3 Chemical composition of H13 steel 25
Table 4 Important process parameters and their level for FSW of AA6082 28
Table 5 Experimental design matrix and results 30
Table 6 ANOVA analysis for tensile strength 32
Table 6 ANOVA analysis for Micro hardness 34
Table 7 FSW parameters 49

Abstract

Friction stir welding (FSW) is a relatively new solid-state joining process. This joining technique is energy efficient, environment friendly, and versatile. In particular, it can be used to join aluminium alloys and other metallic alloys that are hard to weld by conventional fusion welding. It is suitable for joining of Al alloys, Mg alloys, Cu alloys, Ti alloys, steel and joining of dissimilar metals and alloys. AA6082 is a heat treatable alloy with major alloying element is magnesium and silicon. In this study optimization of process parameters (tool rotational speed, welding speed, tool shoulder diameter to pin diameter ratio) for tensile strength and micro hardness of friction stir welded specimen was carried out. A mathematical model was developed for predicting tensile strength and micro hardness of friction stir welded AA6082 alloy using design expert software (version 6.0.5). Three factors, three levels central composite design have been used to minimize the number of experimental conditions. The developed mathematical relationship can be effectively used to predict the tensile strength and micro hardness of AA6082 alloy at 95% confidance level. These optimized parameters is further used to friction stir welding of AA6082 alloy with TiC nano particles. These TiC nano particles are added in welding zone during welding. Test result shows that inclusion of TiC nano particles enhances the weld strength and hardness.

CHAPTER-1

Introduction

Aluminium matrix composites (AMCs) have enhanced properties as compared to their base material. However, their use are limited because they encountered difficulties during machining, forming, and when joined by traditional fusion welding processes [1].Recently particulate reinforced aluminium matrix composites have become a major focus of attention in aerospace, motor sport and automotive industries due to their several attractive advantages over conventional base alloys, such as high specific stiffness and strength to weight ratio at room or elevated temperatures, excellent fatigue properties, high formability and improved wear resistance [2, 3]. However, one of the main limitations for the particulate reinforced aluminium matrix composites is the difficulty in using conventional fusion welding methods because of the porosity, hot cracking, segregation and deleterious reactions between the reinforcement particles and liquid aluminium in the fusion zone [4, 5]. Friction stir welding is a promising candidate for joining particulate reinforced aluminium matrix composites since this method is a solid state process, therefore, the formation of brittle solidification products are not easily produced, the energy input and distortion are significantly lower than in fusion welding techniques, thus improving the welding properties. Most of the previous studies on the joining of particulate reinforced aluminium matrix composites have dealt with gas shielded metal arc welding [6], laser welding, gas tungsten arc welding [4], electron beam welding [4] and friction welding but now friction stir welding is widely used for making joint of aluminium matrix composites [7-10].

Friction stir welding (FSW) is a relatively new solid-state joining technique which eliminated most of the problems that are encountered during conventional fusion arc welding. Low distortion, low energy consumption, high quality joints, better fatigue property, lower residual stresses, fewer weld defects, no harmful emission, high level of dimensional stability, repeatability and low production cost makes FSW an important solid-state joining process. It has expanded rapidly since it was invented at, The Welding Institute (TWI) of UK in 1991 [11].

The basic concept of FSW is very simple. A non-consumable rotating tool with a specially designed pin and shoulder is inserted into the abutting edges of sheets or plates to be joined and traversed along the line of joint. The two primary functions of tools are

(a) Heating of work piece

(b) Stirring/ intermixing of material to produce the joint.

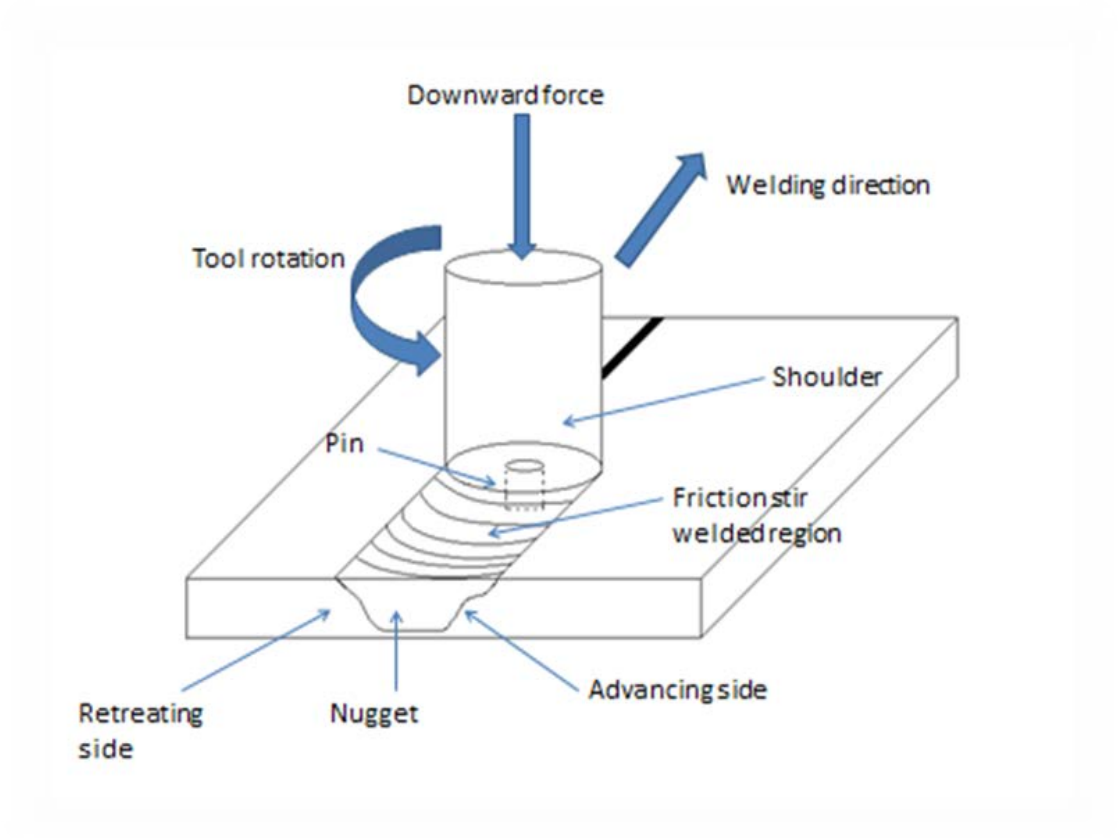

Figure 1- Schematic diagram of FSW

The heating is accomplished by friction between the tool and the work piece. During FSW process, the material undergoes intense plastic deformation at elevated temperature, resulting in the generation of fine and equiaxed recrystallized grains [12]. Heat generated by friction and deformation brings the material into a malleable state that promotes the forward displacement of the tool with the material flowing from the front to the back of the tool where it cools down, The weld is asymmetric since on one side of the weld, called the advancing side, the rotation of the tool is parallel to the advancing direction, while on the other side called the retreating side,

the rotation is opposite to the direction of translation of the tool. The stirring of the tool minimises the risk of having excessive local amounts of inclusions, resulting in a homogenous and void-free weld. Since the amount of heat supplied is smaller than during fusion welding, heat distortions are reduced and thereby the amount of residual stresses [13].

The weld quality is very dependent on the welding parameters such as tool rotation rate, the advancing speed and the tool geometry. A FSW joint consists of the various zones involving different microstructures and mechanical properties. The heat affected zone (HAZ) is the most distant from the joint center line. It is not deformed during the process but the microstructure evolves due to the welding thermal cycles, influencing the mechanical properties. The thermo-mechanically affected zone (TMAZ) and the nugget or stir zone (SZ) are highly deformed by the material rotational flow. The grains in the SZ are equiaxed with a much smaller size (several μm) than the base material. Under some welding conditions so-called onion rings are observed in the SZ [14].

Friction stir welding has been initially developed for welding of Al alloys but other materials have been successfully joined with this process, such as copper, magnesium, titanium, thermo-plastics, steel and stainless steel. Welding of dissimilar materials is a very attractive application of the FSW process. Efforts have been recently devoted to join different Al alloys or Mg alloys. Major advantage of FSW is its ability to weld alloys that are difficult or impossible to weld using fusion welding techniques. For these and many other reasons, FSW has become an alternative technique to be used in high strength alloys that were difficult to join with conventional joining techniques. FSW is also an environment friendly and energy efficient process that requires no filler material and in most cases does not require the use of a shielding gas [11].

As the need for strong, lightweight, high corrosion resistance, high thermal and electrical conductivity, hot and warm formability materials has steadily been increasing, there has also been a growing interest in Aluminum Alloys which possess such properties like that found in age-hardenable Al–Mg–Si alloy. The 6xxx-group of Aluminum Alloys (AA) contains magnesium and silicon as the major alloying elements. Al–Mg–Si alloys have recently been used for automotive body sheet panel for weight saving [12]. In spite of the importance of 6xxx series AA to various

industries a limited number of research work have been devoted to FSW of this series. Koumoulosa et al. [15] studied the FSW of AA6082-T6 and find that welding process softens the material, since the weld nugget is the region where the most deformations are recorded. Scialpi et al. [16] suggested that Tool with cavity and fillet can be considered the best tool for FSW of 6082-T6. Ehab A. El-Danaf et al. [12] reported that welding of 6082 AA-T651 results in softening in the stir zone (SZ) and TMAZ being more significant. This negative effect on the welded joints strength and hardness can be partially recovered by post weld heat treatment PWHT. Cavaliere et al. [17] find that AA6082 friction stir welded with the advancing speed of 115mm/min exhibited the best fatigue properties and the higher fatigue limit. H.J.liu et al. [18] reported that the tensile strength of FS Welded 6061-T6 aluminum alloy defect free joint increases with the welding speed and maximum tensile strength is equivalent to the 69% of that of base material. Many studies that have focused on the FSW of 6xxx AA series alloys were devoted for the 6061 and 6063 alloys, but limited attention was given to particularly the 6082 alloy. Aluminium alloy 6082 is a medium strength alloy with excellent corrosion resistance. It has the highest strength of the 6000 series alloys. Alloy 6082 is known as a structural alloy. As a relatively new alloy, the higher strength of 6082 has seen it replace 6061 in many applications the addition of a large amount of manganese controls the grain structure which in turn results in a stronger alloy. AA6082 has very good weldability but strength is lowered in the weld zone. Applications of AA6082 are typically used in highly stressed applications, Trusses, Bridges, Cranes, Transport applications, Beer barrels etc.

1.1 Material flow and mechanism of joining

Recent literature and experimental works have provided significant insight about several features of materials flow during FSW and the joining process. Material flow occurs through the retreating side and the transport of the plasticized material behind the tool forms the welded joint. Three types of flow affect the overall transport of plasticized materials during FSW.

- First a slug of plasticized material rotates around the tool. This motion is driven by the rotation of the tool and the resulting friction between the tool and the work-piece.

- Another rotational motion of the threaded pin tends to push material downward close to the pin which drives an upward motion of an equivalent amount of material somewhat farther away.
- There is a relative motion between the tool and the work-piece. The overall motion of the plasticized material and the formation of the joint results from the simultaneous interaction of these three effects.

Several plastic flow models have been developed for understanding the material flow phenomena of FSW. These have been used to predict velocities around the tool pin. The velocities have also been estimated from strain rates which, in turn, were obtained from the correlation between grain-size and strain rate [19]. Comparison of the shape of the TMAZ predicted by flow models with microstructural observation has shown satisfactory match. Good agreement between the torque values obtained using dynamometers and the computed values from the flow models for 304L stainless steel [20],1018 Mn steel [21] and Ti–6Al–4V alloy [22] indicates the usefulness of the models to understand the FSW process. Since torque is a measure of the shear stress on the tool and since the shear stress on the work-piece is responsible for both heat generation [23] and plastic flow, validation of the model predictions by experiments indicates that it is appropriate to use the models for the estimation of several important parameters. Though numerical modeling of plastic flow can aid tool design and the optimization of weld quality, there does not appear to have been an application of models towards the prediction of practical processing maps [24].

Arbegast et al. [25] suggested that resultant microstructure and metal flow features of a friction stir weld closely resemble hot worked microstructure of typical aluminum extrusion and forging. Therefore, the FSW process can be modeled as a metalworking process in terms of five conventional metal working zones:

- Preheat,
- Initial deformation,
- Extrusion,
- Forging, and
- Post heat/cool down

The material flow during FSW is quite complicated and the understanding the phenomena of deformation process is difficult. It is important to point out that there are many factors that can influence the material flow during FSW. These factors

include tool geometry (pin and shoulder design, relative dimensions of pin and shoulder), welding parameters (tool rotation rate and direction, traverse speed, plunge depth, spindle angle), material types, work piece temperature, etc. the material flow within the nugget during FSW consists of several independent deformation processes also. [26]

1.2 Factors Affecting FSW

Friction Stir Welding depends upon various factors that affect the material flow pattern and temperature distribution which in turn affects the microstructural evolution of material.

Few major factors affecting FSW are –

1. Tool Geometry
2. Welding Parameters
3. Joint Design
4. Tool Tilt and Plunge Depth

1.2.1 Tool Geometry

The tool geometry has the highest impact on FSW. The tool geometry plays a critical role in material flow and hence the welding quality and maximum welding speed of the tool depends upon the design of the tool. As mentioned earlier, the tool has two primary functions [27]

a) Localized heating
b) Material flow

The friction between the shoulder and workpiece results in the biggest component of heating. From the heating aspect, the relative size of pin and shoulder is important, and the other design features are not critical. The uniformity of microstructure and properties as well as process loads is governed by the tool design. Generally a concave shoulder and threaded cylindrical pins are used. The concave shoulder profile [28]

a) Acts as an escape volume for the material displaced by the pin
b) Prevents material from extruding out of the sides of the shoulder
c) Maintains downwards pressure and hence good forging of the material behind the tool

1.2.2 Welding Parameters

For FSW, two parameters are very important –

a) Tool rotation rate (how fast the tool rotates in clockwise or counter clockwise direction)
b) Tool traverse speed (how quickly it traverses the interface) along the line of joint.

The rotation of tool stirs and mixes the material around the rotating pin and the translation of tool moves the stirred material from the front to the back of the pin and finishes welding process.

As temperature generated in FSW is due to friction between tool and material, so the higher tool rotation rates generate higher temperature because of higher friction heating and result in more intense stirring and mixing of material. A monotonic increase in heating with increasing tool rotation rate is not expected as the coefficient of friction at interface will change with increasing tool rotation rate. Similarly, the decrease in traverse speed results in generating higher temperatures. These parameters are optimized such that weld will have a sufficiently high heat input to ensure adequate material plasticity but not so high that the weld properties are excessively deteriorated. In addition to the tool rotation rate and traverse speed, another important process parameter is the angle of spindle or tool tilt with respect to the workpiece surface. A suitable tilt of the spindle towards trailing direction ensures that the shoulder of the tool holds the stirred material by threaded pin and move material efficiently from the front to the back of the pin. Further, the insertion depth of pin into the work pieces (also called target depth) is important for producing sound welds with smooth tool shoulders. The insertion depth of pin is associated with the pin height. When the insertion depth is too shallow, the shoulder of tool does not contact the original workpiece surface. Thus, rotating shoulder cannot move the stirred material efficiently from the front to the back of the pin, resulting in generation of welds with inner channel or surface groove. [29-31].

1.2.3 Joint Design

The most common joint configurations for FSW are butt and lap joints. In butt joint, two plates or sheets with same thickness are placed on a backing plate and clamped firmly to prevent the abutting joint faces from being forced apart. In lap joint, two

lapped plates or sheets are clamped on a backing plate. A rotating tool is vertically plunged through the upper plate and into the lower plate and traversed along desired direction, joining the two plates. In order to produce effective friction stir welded lap joints sufficient metallurgical and mechanical properties must be obtained by a nugget area as wide as possible together with satisfactory nugget integrity [29]. Cylindrical pins allow obtaining large nugget areas because of the large area they present at the sheet–sheet interface. Apart from butt and lap joint configurations, other types of joint designs, such as fillet joints, are also possible as needed for some engineering applications. Preheating or cooling can also be important for some specific FSW processes. For materials with high melting point such as steel and titanium or high conductivity such as copper, the heat produced by friction and stirring may be not sufficient to soften and plasticize the material around the rotating tool. Thus, it is difficult to produce continuous defect-free weld. In these cases, preheating or additional external heating source can help the material flow and increase the process window. On the other hand, materials with lower melting point such as aluminium and magnesium, cooling can be used to reduce extensive growth of recrystallized grains and dissolution of strengthening precipitates in and around the stirred zone [30].

1.2.4 Tool Tilt and Plunge Depth

A suitable tilt of the spindle towards trailing direction ensures that the shoulder of the tool holds the stirred material by threaded pin and move material efficiently from the front to the back of the pin. Tilting the tool by 2–4 degrees, such that the rear of the tool is lower than the front, has been found to assist this forging process.

The plunge depth is defined as the depth of the lowest point of the shoulder below the surface of the welded plate and has been found to be a critical parameter for ensuring weld quality [31]. The insertion depth of pin is associated with the pin height. When the insertion depth is too shallow, the shoulder of tool does not contact the original workpiece surface. Thus, rotating shoulder cannot move the stirred material efficiently from the front to the back of the pin, resulting in generation of welds with inner channel or surface groove. When the insertion depth is too deep, the shoulder of tool plunges into the workpiece creating excessive flash. In this case, a significantly concave weld is produced, leading to local thinning of the welded plates.

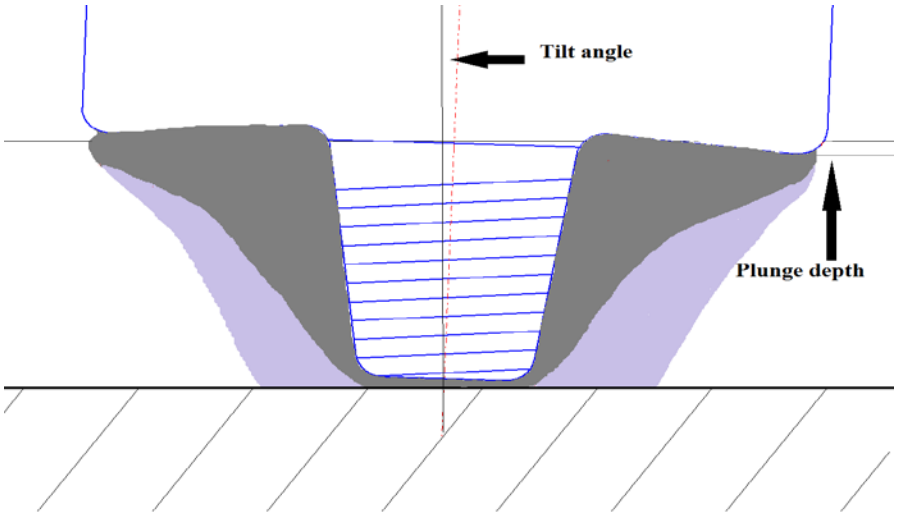

Figure 2 - Plunge depth & Tilt angle

CHAPTER-2

Literature review

Aluminum alloys reinforced with variety of hard ceramic particles are generally known as aluminum matrix composites (AMCs). AMCs are progressively replacing conventional monolithic alloys in several applications due to low density, high specific stiffness and strength to weight ratio, low thermal expansion and improved creep and wear resistance. AMCs play a major role in aircraft, automotive and marine industries. Earlier Al_2O_3 and SiC ceramic particles were predominantly used as reinforcements [32, 33]. But now new kind of AMCs reinforced with SiO_2, TiO_2, AlN, Si_3N_4, TiC, B_4C, TiB_2 and ZrB_2 also developed. The widespread applications of those AMCs are limited due to inadequate development of secondary processes such as machining and joining [34].

Ni et al. [35] investigated the friction stir welding (FSW) of 3 mm thick rolled SiCp/AA2009 sheet in T351 condition. FSW generated high residual stresses in the weld center. Sound FSW joints were achieved with a joint efficiency of 77% and Heat affected zone (HAZ) showed the lowest hardness in the FSW joints. FSW resulted in tensile residual stresses in the weld, with a peak value of about 54 MPa in the weld center. The tensile residual stresses decreased from the centerline to both the Retreating side (RS) and Advancing side (AS), and they reached about 70 MPa in the HAZ. Base metal (BM) showed longer fatigue lives than the FSW joint at higher stress amplitudes of above 150 MPa, but Both the BM and FSW samples showed an equivalent fatigue life at lower stress amplitudes of below 150 MPa. The fatigue samples fractured randomly on the AS and RS of the FSW joint. Fatigue fracture occurred in the HAZ at higher stress amplitudes, which tended to move toward the NZ at lower stress amplitudes. Fatigue cracks tended to initiate at the agglomeration of SiCp at higher stress amplitudes In the BM, while they tended to form at inclusions at lower stress amplitudes. However in the FSW joint neither SiCp agglomeration nor inclusions were observed in the initiation zone, and this region was mainly characterized by the formation of Al dimples.

Kumar et al. [36] attempted to develop a regression models to predict the Ultimate Tensile Strength (UTS) and Percent Elongation (PE) of the friction stir welded (FSW) AA6061 matrix composite reinforced with aluminium nitride particles (AlNp). Statistical software SYSTAT 12 and statistical tools such as analysis of variance (ANOVA) have been used to validate the developed models. FSW process parameters were optimized to maximize UTS of friction stir welded AA6061/AlNp composite joints. After conformity tests this models were found to be accurate. UTS and PE of the friction stir welded joints were influenced by parameters such as tool rotational speed, welding speed, axial force and percentage of reinforcement. Tensile strength(UTS) of the joint fabricated using the optimized FSW parameters is found to be maximum. UTS and PE of FSW joint made with optimized parameters condition is about 1% greater and 9.1% lesser than that of FSW joint made as per the design matrix. Joint efficiency of friction sit welded composite reaches to 94.28% which is 1% greater than the joint efficiency of FSW composite made as per design matrix.

Minak et al. [37] investigated the fatigue Resistance of FSW joints on an as-cast particulate reinforced aluminium based composite (AA6061/22 vol.%/Al_2O_3p) at different welding parameters and the effects of welding on microstructure, tensile and fatigue strength of joint were also investigated. Welded zones appeared substantially defect free and significant reduction of the reinforcement particles also found. Hardness of the FSW zone is always increased from the base material due to the concurrent effect of refinement of the aluminium alloy matrix grain size and embedding. The tensile tests showed a very high joint efficiency, evaluated with respect to the UTS, for all the FSW specimens, significantly higher than that generally measured on composites welded by fusion processes. The fatigue data showed a high spread, both for the base MMC and for all the specimens welded under different process parameters. The slight differences in the fatigue behaviour of the FSW specimens belonging to different sets with respect to the base material was explained by the different microstructural homogeneity from the base to the FSW zones.

Uzun et al. [38] checked the feasibility of friction stir welding (FSW) for joining of AA2124/SiC/25p composite materials. Microhardness, microstructure, EDX analysis and electrical conductivity measurements have been done to evaluate the weld zone characteristics of friction stir welded AA2124/SiC/25p composites. Weld nugget zone shows the relatively homogeneous distribution of SiC particle. The thermo-

mechanically affected zone (TMAZ), which is adjacent to the weld nugget, has been plastically deformed and thermally affected. TMAZ exhibits the elongated grains of Al alloy matrix and the SiC particle-free regions of the composite. The heat affected zone (HAZ) between TMAZ and unaffected base composite regions exhibit a similar microstructure both at the retreating and advancing sides as the base composite. EDX analysis clearly show that both the parent material and the weld region consist of relatively homogeneous distributions of the fine and coarse SiC particles. An average hardness value of parent material is around 250 Hv while the weld nugget has an average hardness of 240 Hv, The average hardness values in the TMAZ are slightly lower than in the weld nugget zone. The electrical conductivity test indicated the presence of friction stir welding seam of the AA2124/SiC/25p composite.

Yigezu et al. [39] investigated the effect of varying process parameters on friction stirred butt welded hot rolled Al + 12%Si/10 wt%TiC in situ composites. A bimetallic tool with flame hardened titanium alloy was used in the experiment. The friction stirred weld zone of Al + 12%Si/10 wt%TiC composite exhibited uniform redistribution of reinforcements with grain refinement in weld zone. The ultimate tensile strength (UTS) and average value of the micro-hardness in the weld zone varied significantly with respect to the process parameters and tool design. The UTS of the FSW joints varied from 124.23 MPa to 171.74 MPa based on the process parameters and tool type. Tool rotational speed of 710 rpm and tool shoulder diameter of 20 mm were preferable welding parameter for better UTS of FSW composite. It was observer that, the developed multiple regression equations satisfactorily predicted the influence of the input variables. The observation exhibited the errors in the test were 0.52–10.41% for UTS, 7.9–9.89% for percentage elongation and 6.99–10.12% for micro-hardness. It was concluded that adopted optimization technique is adequate for the current experimental condition.

Butt joints of 6 mm thick plate of AA6061/B_4C aluminum matrix composite (AMC) is prepared with the help of Friction stir welding (FSW) by Kalaiselvan et al. [40] Friction stir welding of AA6061/B_4C AMC was carried out using a tool rotational speed of 1000 rpm, welding speed of 80 mm/min and axial force of 10 kN. A high carbon high chromium steel with square pin profile tool was used. The weld zone showed homogeneous distribution of B_4C particles with grain refinement. A joint efficiency of 93.4% was realized under the experimental conditions. The hardness of

weld zone was higher than that of parent composite and tensile strength of welded joint was comparable to the strength of the parent composite under the experimental conditions. A joint efficiency of FSW composite reached to 93.4% under the experimental conditions.

Self-support friction stir welding (SSFSW) of 5 mm thick 6082-T6 aluminium alloy was done by Wan et al. [41] The SSFSW tool have upper shoulder in concave shape and the lower shoulder in convex shape, Shape of weld in SSFSW joint differs from the weld made from conventional FSW, and is slightly hourglass shaped. Four distinct zones, heat-affected zone (HAZ), thermo-mechanically affected zone (TMAZ), upper weld nugget zone (UWNZ) and lower weld nugget zone (LWNZ), were presented in the joint due to the introduction of the lower shoulder. Due to an overaging effect and the coarser second phase particles , The average microhardness in the WNZ (UWNZ and LWNZ) near the TMAZ was the lowest . The values of microhardness of the TMAZ were relatively high which reached 89.4 HV and 84.7 HV, respectively, in the upper and lower part of the SSFSW joint on the advancing side. In SSFSW TMAZ is highly deformed due to temperature and deformation. The grain structure in the HAZ is similar with the base material, however, the grain size decreases with increasing distance of the weld centerline.

Byung-Wook AHN et al. [42] produced a friction stir welded (FSW) joint of AA5083/SiC composites and then conducted some metallographic examinations and hardness tests. It was found that the distribution of SiC particles was more homogenous in the stir zone (SZ) after two passes processing than that in the SZ after one pass processing due to the repeated stirring of the joint. Due to the pinning effect by the SiC particles grain size of the SZ with SiC particles was smaller than that of the SZ without SiC particles. Microhardness of the SZ with SiC particles was higher than that of the SZ without SiC particles due to the reduction in the grain size and the presence of the reinforcing SiC particles in the aluminum matrix.

Kumar et al. [43] conducted a friction stir welding of hot rolled Al–4.5%Cu/TiC in situ metal matrix composites by using hardened bimetallic tool with varying shoulder surface geometries and other process variables. A predictive model has been developed to estimate the weld properties such as tensile strength and ductility. The X-ray diffraction (XRD) analysis indicated formation of $CuAl_2O_4$ and $CuAl_2$ to some

extent in the stir zone of Al–4.5%Cu/TiC butt welds. Fractography of the weld samples revealed ductile nature of fracture. Weld strength of 89% that of the base material was achieved through multi response optimization of the welding parameters and tool geometry. 1 mm flat shoulder surface with concavity of 7˚ tool and 500 rpm tool rotational speed were preferable welding parameter for better tensile strength (UTS) and elongation (EL) (%) of the butt joints. The SEM micrograp observed fairly redistribution with fine grain refinement of TiC reinforcements in the weld zone. The other observation was that, the developed multiple regression equations satisfactorily predicted the influence of the input variables. The observed errors in the test cases were 1.36–6.66% for UTS and 1.02–7.23% for EL (%).The microhardness values measured across the weld zones exhibited maximum and minimum at stir zone (SZ) and heat affected zone (HAZ) respectively.

El-Danaf et al. [44] conducted a Friction stir welding of 6082 AA T651 using three different combinations of tool feed rates (90, 140 and 224 mm/min) and tool rotational speeds (850, 1070 and 1350 rpm) and extracted the conclusions that due to dissolution of β' and β" second phase particles considerable loss in hardness in the stir zone (SZ) and thermo-mechanically affected zone (TMAZ) is occurred. This negative effect on the welded joints hardness and strength can be partially recovered by PWHT. A post weld heat treatment (PWHT) of 175˚C for 5 and 12 h was given to the weld joints for all welding conditions and the mechanical properties and microstructure were re-evaluated. The hardness and strength were partially recovered due to re-precipitation of the β" precipitates. Prolonged PWHT at 175 ˚C for 12 h on 6082-AA is more influential in recovering the joint's strength. The response to PWHT of samples welded at higher welding speeds is less pronounced than that welded at lower speeds. This observation could be attributed to the almost complete dissolution of second phase particles with lower welding speeds due to the higher heat input which means that there are more solutes in the matrix available for re-precipitating the second phase. The grain size for all welding conditions ranged from 2.3 to 2.8 μm. The variation of grain size among the different welding conditions and also after PWHT is marginal.

Kwon et al. [45] investigated the friction stir welding of 2 mm thick 5052 aluminium alloy plates. The tool rotation speeds were ranging from 500 to 3000 rpm under a constant traverse speed of 100 mm/min. Welded joints were obtained at tool rotation

speed 1000, 2000 and 3000 rpm. At 500, 1000, and 2000 rpm onion ring structure was clearly observed in the friction-stir-welded zone (SZ). The effect of tool rotation speed on the onion rings was observed. Grain size in the SZ is smaller than that in the base metal and is decreased with a decrease of the tool rotation speed. The study showed that the strength, tensile strength of the joint is more than that of the parent metal. The investigation also demonstrated that the joint is less ductile than the parent alloy.

The study conducted by CAO et al. [46] was aimed at studying whether the extreme temperature in the work piece can extent the lower bound of the melting temperature range and trigger liquation during friction stir welding (FSW) of aluminium alloys which was observed in some computer simulation. AA 2219, an Al-Cu alloy was the work piece material due to its clear lower bound of the melting temperature array which is the eutectic temperature 548°C. Besides FSW, gas metal arc welding (GMAW) of Alloy 2219 was also accompanied to provide a benchmark for checking liquation in FSW of Alloy 2219.The study under both optical and scanning electron microscopy revealed found that in GMAW of Alloy 2219 (Al_2Cu) particles performed as in-situ micro sensors, which indicates liquation due to reaction between CU and Al forming eutectic particles upon reaching the eutectic temperature. But in FSW, no evidence of q-induced liquation was found suggesting that the eutectic temperature was not reached.

Adamowski et al. [47] analyzed the mechanical properties and microstructural variations in Friction Stir Welds in the AA 6082-T6 with varying process parameters. Tensile test of the welds was done and relation among the process parameter was judged. Microstructure of the weld interface was observed under optical microscope. Also micro hardness of the resulting joint was measured. It was observed that test welds show resistance to increment of welding speed, Hardness reduction was observed in weld nugget and heat affected zone (HAZ). The reason for this occurrence was the kinetic and thermal asymmetry of the FSW process. An initial stage of a longitudinal, volumetric defect was found at the interface of weld nugget and TMAZ. The hardness was inferior to that of fusion welding. Tunnel (worm hole) defects were found in the nugget zone.

LIU et al. [48] studied the characteristics of friction welding characteristics of AA 2017-T351 sheet in which they found that the relation between the parameters and also they have studied the microstructure of the weld joints. Graphs between revolutionary pitch and strength, distance from weld center and Vickers Hardness, revolutionary pitch and fracture location at the joints were plotted. From the hardness test and tension tests it was deducted that FSW makes the material soft and it also decreases the tensile strength of the material. Microscopic analysis confirms the generations of fractures in the joint at the interface among weld nugget and thermodynamically affected zone.

Vural et al. [49] scrutinized the friction stir welding competency of the EN AW 2024-0 and EN AW 5754-H22 Al alloys. These two aluminium alloys are extensively used in the industry. The experiment presented that the hardness value of EN AW 2024-0 at the weld area is increased about 10-40 Hv. This may be the result of recrystallization and compact grain structure formation. But hardness of EN AW 5754-H22 got decreased due recrystallization and loose grain structure formation. Welding performance of EN AW 2024-0 is 96.6 and for EN AW 5754-H22 it is 57%. Welding performance of dissimilar Aluminium alloys EN AW 2024-0 and EN AW 5754-H22 is reached a value of 66.39%. Analysis of Welding zone using scanning electron microscope showed no change in the microstructure in the welding zone. Hardness distribution at the weld zones didn’t show any significant change in hardness.

Nandan et al. [50] reviewed the recent trends in FSW process, weldment structure and properties of the resulting material at the weld joints. This study dealt with the essential understanding of the process and its consequences in the molecular level. Other characteristics that are studied are heat generation, heat transfer and plastic flow during welding, components of tool design, study of defect formations and the structure and properties of the welded materials. They described important factors that have to be optimized to reduce fracture and improve the uniformity of weld properties so that FSW can be expanded to new engineering fields. Principles of heat transfer, material flow, tool-work–piece contact conditions and properties of various process parameters, efficient tools have been formulated. Uncertain parameters of FSW like friction coefficient, the extent of slide between the tool and the work–piece, the heat transfer coefficients for different work–piece surfaces, splitting of the heat amongst

the work–piece and the tool at the tool-work piece boundary are also counted for and processes to optimize these parameters are discussed.

The weld ability of AA 5083-H111 (non-heat treatable) and AA 6082-T6 (heat treatable) Aluminium alloys, that are extensively used in welding production is inspected by Rodrigues et al. [51] The work pieces were welded under broad range of FSW parameters (changing tool dimensions, rotation and traverse velocities, axial force and incline angles) to ensure high welding speeds. The welds defects and weld strength were analyzed and compared to the distinctly different plastic behaviours of both base materials. The study proved that high traverse speed can be achieved with proper tool parameters, base material characteristics and plate thickness. It was shown that founding suitable axial force values rests intensely on base material characteristics. It was determined that the mechanical properties of the non-defective welds are relatively independent of the welding conditions. For AA 6082 alloy, the use of very high welding speeds ascertained to be very operative in evading extra softening in the HAZ, with positive values in weld yield strength productivity.

Yazdanian et al. [52] scrutinized the effect of pin length, welding speed and rotation rate on the weld strength using AA 6060 as work piece for FSW. The major factor in determining the weld strength is the rotation speed of the tool. Higher rotation rate made the joint weak and vice versa. Effect of rotation speed on heat generation and material flow was also enlightened. It was found that higher rotation rate may result in larger interface lifting and hence higher degree of hooking, reducing the effective weight bearing area.

Merzoug et al. [53] described the main parameters of Friction stir spot welding (FSSW). The parameter under consideration is shape of the tool. It is established that shape of tool decides the resistance of the joint of welding. This may be due to the heat gradients and mechanical stresses experienced by material throughout welding. The nature of material and the selection of the parameters (geometry, positioning, tool rotating, penetration depth and the force applied of the pin and the shoulder) also decide the heat generation and the strength of the weld joint.

The effect of process constraints (cycle time, tool speed and axial force) on the sample temperature that is measured 2 mm away from the weld in spot friction welding (SFW) of Al 6111-T4 was investigated by Arul et al. [54] They tried to

correlate temperature with shear load. It was found that the maximum lap shear load should be greater than 2.5 kN and temperatures should be larger than a threshold value (350 Centigrade at a location close to the SFW joint in the experiment) to achieve decent joint strength. During microstructure analysis two internal welds geometric structures at the cross section area were identified which were may be due to the shear and mixed failure modes of the lap shear tested samples. A model was settled and corroborated using experimental data of the cross section area of SFW joint with either shear or mixed mode fracture that forecasted that SFW joint strength is maximized at the transition region between the shear and mixed mode fracture.

Friction stir welding of different materials was done by Muruganandam et al. [55] for four different tool rotation speeds namely 600, 800, 1000 and1200 rpm. Radiology was done to study the defects in the weld joint. The analysis indicated that defect concentration was higher for the 600 rpm tool rotation. It was a little reduced for 800 rpm and even lesser for the 1000 rpm speed rotation. Least defects were found at the highest rpm (1200).

Friction welding of austenitic stainless steel (AISI 304) and optimization of the welding parameters to establish weld quality was done by Sathiya et al. [56] Austenitic stainless specimens were welded using the laboratory model friction welding machine. Aural emission originated during the tension test from the joints was acquired to evaluate the quality of the joints. They also proposed a genetic algorithm to decide near optimal configurations of process parameters. The tensile tests showed that the weld joints exhibited similar strength with the base material. The post welding analysis showed increase in hardness due to recrystallization. Micro vicker's hardness increases with increasing friction time may be due to the heating of material at the weld region. The objective function is formulated by regression analysis. Genetic Algorithm is then applied to the objective function for optimizing the process parameters. The minimum difference observed between theoretical and the experimental values confirm the applicability of GA for the friction welding process.

Rotary friction welding of AA1050 aluminium and AISI 304 stainless steel was performed and tensile tests, Vickers microhardness, metallographic tests and SEM-EDX analysis etc. were conducted to assess the effect of weld parameters on

microscopic as well as physical properties of the weld joint by Paduan Alves et al. [57] Joints were acquired with greater mechanical properties of the AA1050 aluminum, with fracture arising in the aluminum away from the bonding boundary. The inspection by EDX at the interface of the junction presented that inter-diffusion occurs between the main chemical components of the materials involved.

Kumaran et al. [58] carried out friction welding of tube to tube plate using an external tool and optimized the process parameters by Taguchi L8 orthogonal array. The arrangement of the process parameters was obtained and ANOVA had been accompanied to predict the statistical importance of the process parameters. They implemented Genetic Algorithm (GA) to optimize the parameters. The real-world viability of applying GA to friction welding process was ensured by studying the eccentricity between forecasted and experimentally acquired friction welding process parameters

Lakshminarayanan et al. [59] had done a Comparison between Response Surface Methodology (RSM) with Artificial Neural Network (ANN) for predicting tensile strength of friction stir welded AA7039 aluminium alloy joints. Two models were developed by using design of experiments (DOE) for predicting tensile strength of friction stir welded AA7039 aluminium alloy. They concluded that Rotational speed is the factor that has greater influence on tensile strength, followed by welding speed and axial force. A maximum tensile strength of 319 MPa is exhibited by the FSW joints fabricated with the optimized parameters of 1460 rpm rotational speed, 40 mm/min welding speed and 6.5 kN axial force. ANN model can better predict the tensile strength of welded joint within the range that they had been trained. The results of the ANN model indicate it is much more robust and accurate in estimating the values of tensile strength when compared with the response surface model.

Ericsson et al. [60] studied the Influence of welding speed on the fatigue strength of friction stir welded Al–Mg–Si alloy 6082 and compared it with the fatigue strength of joint made by MIG and TIG welding. The fatigue strength of Friction Stir welded Al–Mg–Si alloy 6082 is higher than that of MIG-pulse and TIG welds of the same material. The TIG welds show better fatigue performance than MIG. Mechanical and fatigue properties of the FS welds are relatively independent of welding speed in the range of low to high commercial welding speed in this alloy. An extra low speed gave

improved properties. Welds in the artificially aged condition T6 showed equivalent fatigue properties. Contributing factors to this behaviour are the higher ductility in the T6 condition, which reduces the influence of stress concentrations and that crack propagation in the T6 condition mainly takes place in the HAZ. The softening behaviour around FS weldments was modelled and a fair representation of the measured hardness profiles as a function of welding speed was found.

Thermoelasticity stress analysis and CCD camera analysis of crack propagation in AA6082 friction stir welded joints was conducted by Cavaliere et al. [61] The rotating speeds and advancing speeds of the threaded tool were 1600 RPM, 230, 325, 460 mm/min and 1000 RPM, 165, 230 and 325 mm/min, respectively. The joints welded with a rotation speed of the tool of 1600 RPM and a travel speed of 230 mm/min showed the highest fatigue resistance, the samples welded at 1600 RPM 325 mm/min and 1000 RPM 165 mm/min experienced a very similar behaviour at high stress amplitude. The fatigue crack rate for all the joints showed that the joints welded with a rotating speed of 1000 RPM are more sensitive to crack initiation respect to the ones obtained at 1600 RPM. In addition the joints welded at 1600 RPM show a crack growth rate lower than those welded with a rotating speed of 1000 RPM.

Study of fatigue behaviour of AA6082 friction stir welds under variable loadings was done by Costa et al. [62] study suggested that In friction stir welds the tunnel defects and shear lips lead to fatigue life reduction. Tunnel defects considered to be more detrimental to fatigue resistance than stress concentration. Therefore to enhance the fatigue strength of friction stir weld it is crucial to avoid the presence of tunnel and other severe weld defects. Although residual stresses were not measured in this work, the small test samples (160 × 15 × 4 mm) tested transversely implies that these stresses must be very small.

Moreira et al. [63] made a comparison between fatigue crack growth in friction stir welds of 6082-T6 and 6061-T6 aluminium alloys. For both alloys crack propagation rates of the friction stir welded material are lower than the crack propagation rates of base material. This behaviour is related to the compressive residual stresses developed at crack vicinity when propagating in friction stir material. However two base materials show very similar crack propagation rates but 6061-T6 friction stir material is more resistant to crack propagation than 6082-T6 friction stir material.

CHAPTER-3

Experiment -1 Optimization of tensile strength of friction stir welded AA6082 by Response surface methodology (RSM).

3.1 Introduction

Response surface methodology (RSM) is a collection of mathematical and statistical techniques for empirical model building. By careful design of experiments, the objective is to optimize a response (output variable) which is influenced by several independent variables (input variables). An experiment is a series of tests, called runs, in which changes are made in the input variables in order to identify the reasons for changes in the output response.

Friction stir welding(FSW) is an innovative solid state joining technique and has been employed in aerospace, rail, automotive and marine industries for joining aluminium, magnesium, zinc and copper alloys. The FSW process parameters such as tool rotational speed, welding speed, axial force, tool shoulder and pin diameter play a major role in deciding the joint characteristics. Response surface methodology was used to predict the tensile strength of friction stir welded AA6082-T651 aluminium alloy. The experiments were conducted based on three factors, three-level, and central composite, face centered design with full replications technique, and mathematical model was developed. The three factors namely tool rotational speed, welding speed and ratio of shoulder to tool pin diameter were used as input variables.

3.2 Workpiece Material

A commercial 6082-T651 AA plate which is solution heat treated, stress relieved by stretching then artificially aged is used as specimen for FSW. Chemical composition of workpiece material is given in table 1.

Table 1-Chemical composition of AA6082-T651

Element	Si	Mg	Mn	Fe	Cr	Zn	Ti	Cu	other	Al
Wt.%	1.2	.75	.79	.40	.15	.10	.07	.06	.10	Balance

3.3 Tool used

Some of the tool pin profiles analyzed by the researchers are straight and draft type of cylindrical, square, triangular, hexagonal, octagonal and cylindrical threaded. Elangovan et al. [64] attempted to weld AA2219 aluminium alloys by various profile tool pins such as straight cylindrical, taper cylindrical, threaded cylindrical, straight square and straight triangular. It was found that straight square profile pin gave better tensile strength among the other tool pins. Vijay et al. [65] developed the different FSW tool pin profiles viz., straight square, straight hexagon, straight octagon, taper square, taper hexagon and taper octagon with different shoulder to pin diameter (D/d) ratio of 2.8, 3 and 3.2 to weld the in situ Al-6061-10 wt% TiB_2 composite and studied the effect of tool pin profile on metallurgical and mechanical properties of the weldments. It was found that straight square profile tool pin with the D/d ratio of 2.8 shows better joint strength when compared to the other pins.

Three different straight square pin tools are used for friction stir welding as shown in figure3. It was fabricated from H13 hot working steel and heat treated to 58HRC (Hardness, Rockwell C-scale). These tools have square pin on cylindrical shoulder. square pin have 6mm diagonal length and 5.7mm height with different shoulder diameter like 21, 18, 15mm. Tool shoulder and pin diameter is considered one of the important parameter of friction stir welding due to which welding is done on different tool shoulder to pin diameter ratio.(3.5, 3, 2.5).

Table 2-Tool specification

Tool no	Shoulder diameter (mm) D	Pin diagonal (mm) d	D/d
1	21	6	3.5
2	18	6	3
3	15	6	2.5

Table 3- Chemical composition of H13 steel

Element	Cr	Mo	Si	V	C	Ni	Cu	Mn	P	S
Wt.%	1.35	1.50	1.00	1.00	0.45	0.3	0.25	0.40	0.03	0.03

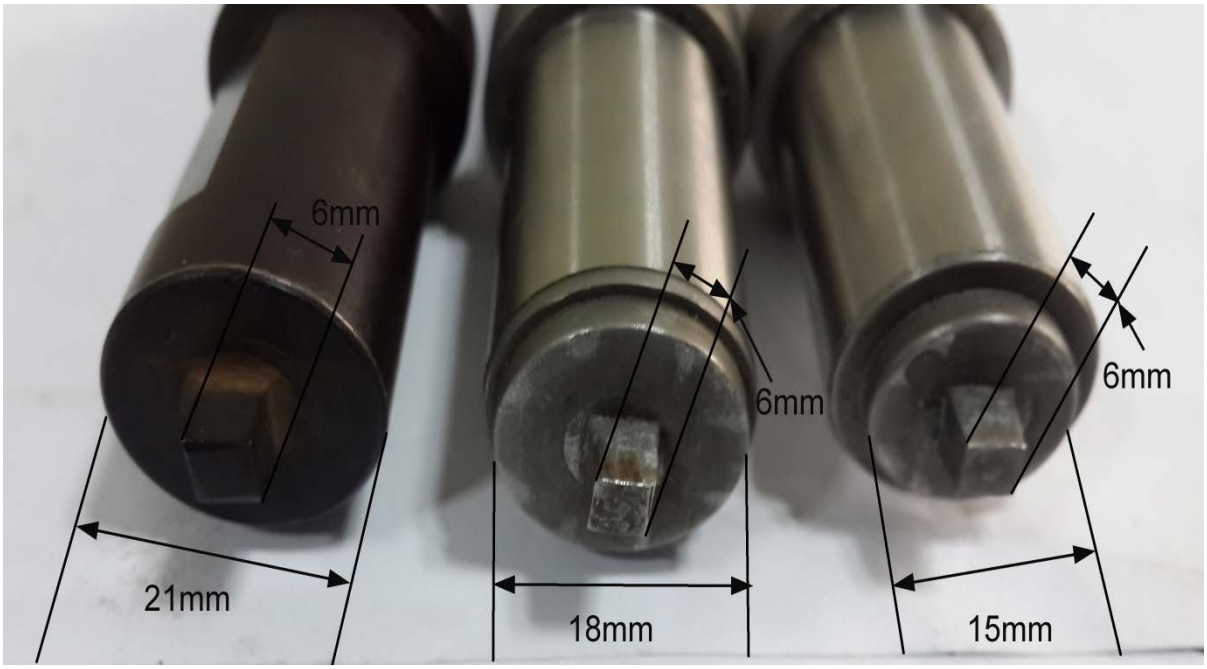

Figure 3 - Tools used for FSW of AA6082

3.4 Experimental setup

An indigenous developed friction stir welding machine (R V machine tools, FSW-4T-HYD) (15 hp; 3 000 rpm; 25 kN) as shown in figure-3 is used for welding process. This machine has a vertical spindle to hold the tool and a fixture with four hydraulic actuated clamps and a backing plate with groove (200mm×80mm) to hold the work piece. Work holding fixture can move in X, Y and Z axis. Groove on backing plate is meant to strongly hold the work piece. Maximum operational speed of spindle is 3000 rpm. Rotational speed, welding speed and tool tilt angle can be altered easily but welding force cannot be changed on this machine.

Figure 4 -Friction stir welding machine

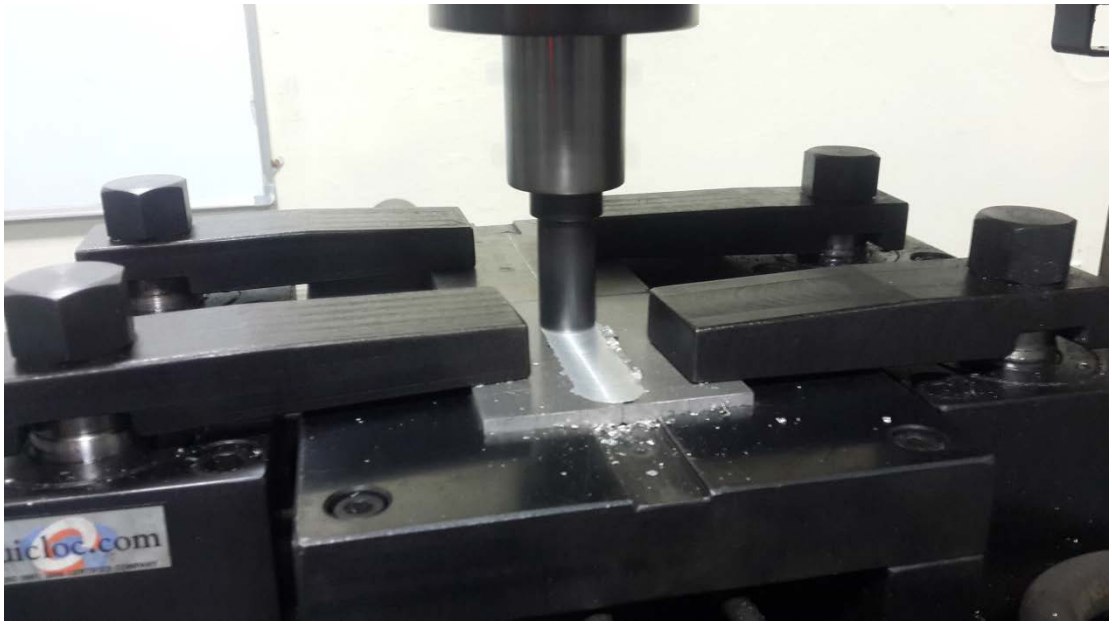

Figure 5 -Tool and work holding device

3.5 Experimental procedure

The 6 mm thick plates were cut into the required sizes (200 mm× 80 mm) by power hacksaw cutting and milling. Square butt joints were prepared by FSW machine

which is mention in section 3.4. A non-consumable rotating tool made of H13 steel was used to fabricate FSW joints. FSW of 20 specimens were performed according to the design of experiment (DoE) which is formed with the help of Design-Expert ® version 6.0.5 software. Different parameters like tool rotational speed (800-1200 rpm), welding speed (30-90 mm/min) and ratio of shoulder and tool pin diameter ((D/d) 2.5-3.5) is used to generate the DoE.

Table 4- Important process parameters and their level for FSW of AA6082

Parameters	Level		
	(-1)	(0)	(+1)
Rotational speed (rpm)	800	1000	1200
Welding speed (mm/min)	30	60	90
Shoulder to pin ratio	2.5	3	3.5

After welding specimen is cut by wire electrical discharge machine (EDM) as per American Society for Testing of Materials (ASTM: B557-06) standard shape which is shown in figure-6. Then tensile test is performed in 100 kN, electro-mechanical controlled universal testing machine at a speed of 1mm/min. This tensile test data is used to optimize the ultimate tensile strength of joint with the help of RSM.

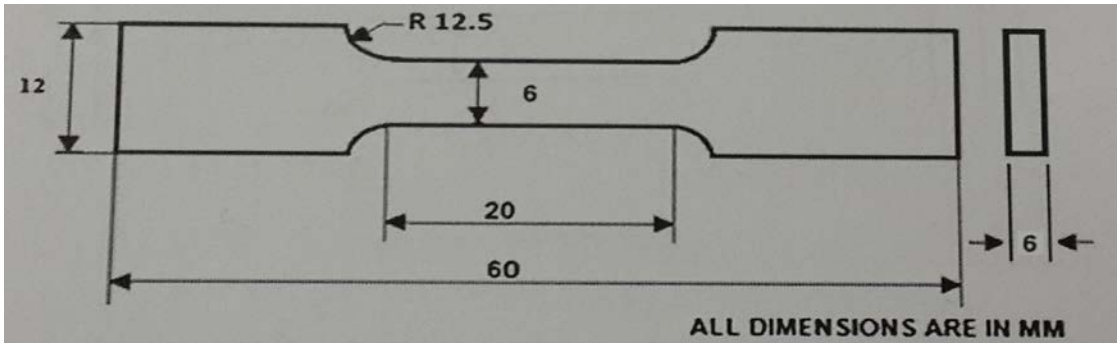

Figure 6-Standard tensile test specimen

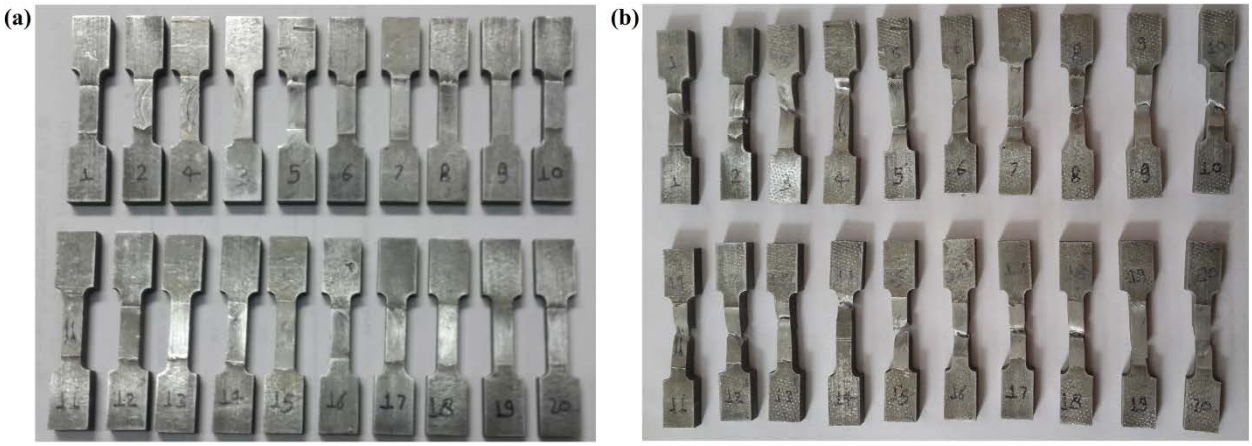

Figure 7 -Tensile specimen (a) before test (b) after test

3.6 Development of mathematical model

3.6.1 Response surface methodology

Response surface methodology (RSM) is a tool which consists of mathematical and statistical technique used for the analysis of those problems in which independent variables like x_1, x_2, x_3,……x_n influence a dependent variable Y or response and the aim is to optimize the response or variable Y. In various experimental conditions ,we can show a relationship between independent factors in quantitative form like ultimate tensile strength of friction stir welded zone depends on various factors like tool design, tilt angle, pin geometry, shoulder diameter to pin diameter ratio, tool material, shoulder geometry, axial force, tool rotation speed, feed rate, material thickness, material melting point temperature etc. These factors can have following type of relationship

$$\boldsymbol{Y = \Phi\{x_1, x_2, x_3 \dots \dots x_n\} + Er} \dots\dots\dots\dots\dots\dots (1)$$

Between the response y and x_1, x_2, x_3,……x_n of n quantitative factors, the function Φ is called response surface or function. The term Er measures the error occurred in experimentations. In this present study, RSM has been applied for development of the mathematical model in the form quadratic model for the quality characteristics of the friction stir welded AA6082 aluminium alloy .In applying the response surface methodology, the independent variables was seen as a surface to which a mathematical model (quadratic) is fitted

The quadratic equation used to represent the response surface Y is given by [66]

$$Y = B_o + \sum B_i x_i + \sum B_{ii} {x_i}^2 + \sum B_{ij} x_i x_j + E_r \ldots\ldots\ldots\ldots\ldots (2)$$

for three factors, selected quadratic model can be expressed as:

$$\sigma = B_o + B_1(A) + B_2(B) + B_3(C) + B_{11}(A^2) + B_{22}(B^2) + B_{33}(C^2) + B_{12}(AB) + B_{13}(AC) + B_{23}(FS) \ldots\ldots\ldots\ldots\ldots\ldots (3)$$

Table 5- Experimental design matrix and results

Code value					Real value			Tensile strength MPa	Micro-hardness Hv (GPa)
Std.	Run	A	B	C	Rotational speed (rpm)	Welding speed (mm/min)	Shoulder to pin ratio (D/d)		
1	18	-1.00	-1.00	-1.00	800.00	30.00	2.50	216	73
2	3	1.00	-1.00	-1.00	1200.00	30.00	2.50	227	76
3	19	-1.00	1.00	-1.00	800.00	90.00	2.50	200	71.8
4	14	1.00	1.00	-1.00	1200.00	90.00	2.50	210	72.4
5	6	-1.00	-1.00	1.00	800.00	30.00	3.50	209	68.4
6	11	1.00	-1.00	1.00	1200.00	30.00	3.50	191	70.8
7	8	-1.00	1.00	1.00	800.00	90.00	3.50	173	76
8	7	1.00	1.00	1.00	1200.00	90.00	3.50	203	75
9	13	-1.00	0.00	0.00	800.00	60.00	3.00	205	70
10	17	1.00	0.00	0.00	1200.00	60.00	3.00	233	80
11	12	0.00	-1.00	0.00	1000.00	30.00	3.00	192	78.8
12	20	0.00	1.00	0.00	1000.00	90.00	3.00	204	97
13	16	0.00	0.00	-1.00	1000.00	60.00	2.50	188	63.2
14	10	0.00	0.00	1.00	1000.00	60.00	3.50	185	64.3
15	4	0.00	0.00	0.00	1000.00	60.00	3.00	192	78.4
16	9	0.00	0.00	0.00	1000.00	60.00	3.00	196	88.8
17	1	0.00	0.00	0.00	1000.00	60.00	3.00	190	88.5
18	5	0.00	0.00	0.00	1000.00	60.00	3.00	196	89.6
19	2	0.00	0.00	0.00	1000.00	60.00	3.00	188	90.2
20	15	0.00	0.00	0.00	1000.00	60.00	3.00	192	89.3

In order to estimate the coefficients, various types of experimental design techniques are available. In this study, central composite face centered design (Table 5) was used which fits the second order response surfaces very accurately. Central composite face centered (CCF) design matrix in which the star points being at the center of each face of factorial space was used, so α= ±1. This design requires three levels of each factor. A CCF design provides comparatively good quality predictions over the entire design space and does not use the points outside the original factor range. The upper limit of a factor was coded as +1, and the lower limit was coded as –1. All the coefficients were determined by applying central composite face centered design using the Design Expert (version 6.0.5) statistical software package. All the significant coefficients were obtained at 95% confidence level.

3.6.2 Model for Tensile strength

After finding out the significant coefficients final model was developed using only these coefficients and the final mathematical model to estimate tensile strength is given as follows:

$$\sigma_1 = 194.55 + 6.10\,(A) - 4.50\,(B) - 8.00\,(C) + 21.14\,(A^2) + 0.14(B^2) - 11.36(C^2) + 5.88\,(AB) - 1.12\,(AC) + 1.12(BC) \ldots\ldots\ldots\ldots\ldots\ldots \quad (4)$$

3.6.3 Checking adequacy of model

Analysis of variance (ANOVA) technique was used to test the adequacy of the developed model and the results of second order response surface model fitting in the form of analysis of variance (ANOVA) are given in Table 5. The determination coefficient (R^2) indicates the goodness of fit for the model. The Model F-value of 3.32 implies the model is significant. There is only a 3.76% chance that a "Model F-Value" this large could occur due to noise.

Values of "Prob > F" less than 0.0500 indicate model terms are significant. In this case C, A^2 are significant model terms. Values greater than 0.1000 indicate the model terms are not significant. If there are many insignificant model terms (not counting those required to support hierarchy), model reduction may improve your model. The "Lack of Fit F-value" of 18.28 implies the Lack of Fit is significant. There is only a 0.31% chance that a "Lack of Fit F-value" this large could occur due to noise. Significant lack of fit is bad, we want the model to fit. A negative "Pred R-Squared"

implies that the overall mean is a better predictor of your response than the current model."Adeq Precision" measures the signal to noise ratio. A ratio greater than 4 is desirable. Our ratio of 6.625 indicates an adequate signal. This model can be used to navigate the design space. The value of adjusted determination coefficient (adjusted R^2=0.5236) is also reasonable, which indicates a significance of the model. Adequate precision compares the range of predicted values at the design points to the average prediction error. At the same time a relatively lower value of the coefficient of variation (4.99) indicates improved precision and reliability of the conducted experiments. The value of probability >F in Table 5 for model is less than 0.05, which indicates that the model is significant. In the same way, rotational speed (A), welding speed (B) and shoulder diameter to pin diameter ratio (C), interaction effect of rotational speed with welding speed, interaction effect of rotational speed with shoulder diameter to pin diameter ratio (AC), interaction effect of welding speed with shoulder diameter to pin diameter ratio (BC) and second order term of rotational speed (A), welding speed (B) and axial force (C) have significant effect.

Table 6-ANOVA analysis for tensile strength

Source	**Sum of Squares**	**D_f**	**Mean SquareValue**	**F-value**	**Prob > F**
Model	2957.34	9	328.59	3.32	0.0376
A	372.10	1	372.10	3.76	0.0812
B	202.50	1	202.50	202.50	0.1831
C	640.00	1	640.00	6.47	0.0292
A^2	1228.55	1	1228.55	12.41	0.0055
B^2	0.051	1	0.051	5.167E-004	0.9823
C^2	355.11	1	355.11	3.59	0.0874
AB	276.13	1	276.13	2.79	0.1258
AC	10.12	1	10.12	0.10	0.7557
BC	10.13	1	10.13	0.10	0.7557
Residual	989.66	10	98.97		
Lack of Fit	938.33	5	187.67	18.28	0.0031
Pure Error	51.33	5	10.27		
Corrected	3947.00	19			

Total		
Standard Deviation	9.95	R^2 = 0.7493
Mean	199.50	Adjusted R^2=0.5236
Coefficient of variation	4.99	Predicted R^2=-1.9578
Press	11674.54	Adequate R_2=6.625

3.6.4 Model for Microhardness

The hardness of composite surface was quantified using micro-indentation at a load of 1.96N. Cubic blocks with dimensions of 12mm×10mm×4mm were machined out of the AA6082 surface for micro-hardness testing. They were fine polished. Both dry and wet polishing was performed. After finding out the significant coefficients final model was developed using only these coefficients and putting these coefficients obtained for microhardness analysis in Eq.3 model equation will be

$$\text{Microhardness } \sigma_2 = \{+84.38 +1.50(A) +2.52(B) -0.19(C) -4.75 (A^2) +8.15(B^2) - 16.00(C^2) -0.73(AB) -0.28(AC) +2.07(BC)\} \ldots\ldots\ldots\ldots\ldots\ldots (5)$$

3.6.5 Checking adequacy of model

Analysis of variance (ANOVA) technique was used to test the adequacy of the developed model and the results of second order response surface model fitting in the form of analysis of variance (ANOVA) are given in Table 5. The determination coefficient (R^2) indicates the goodness of fit for the model. The Model F-value of 3.29 implies the model is significant. There is only a 3.88% chance that a "Model F-Value" this large could occur due to noise. Values of "Prob > F" less than 0.0500 indicate model terms are significant. In this case C^2 are significant model terms. Values greater than 0.1000 indicate the model terms are not significant. If there are many insignificant model terms (not counting those required to support hierarchy), model reduction may improve your model. The "Lack of Fit F-value" of 3.35 implies the Lack of Fit is not significant relative to the pure error. There is a 10.52% chance that a "Lack of Fit F-value" this large could occur due to noise. Non-significant lack of fit is good we want the model to fit. A negative "Predicted R^2" implies that the overall mean is a better predictor of our response than the current model. "Adequate Precision R^2" measures the signal to noise ratio. A ratio greater than 4 is desirable. Your ratio of 6.420 indicates an adequate signal. This model can be used to navigate

the design space. Adjusted R^2= 0.7474 is also reasonable which indicates the significance of the model.

Table 7-ANOVA analysis for Micro hardness

Source	Sum of Squares	D_f	Mean Square Value	F-value	Prob > F
Model	1293.13	9	143.68	3.29	0.0388
A	22.50	1	22.50	0.51	0.4895
B	63.50	1	63.50	1.45	0.2558
C	0.36	1	0.36	8.260E-003	0.9294
A^2	62.17	1	62.17	1.42	0.2605
B^2	182.46	1	182.46	4.17	0.0683
C^2	704.40	1	704.40	16.12	0.0025
AB	4.20	1	4.20	0.096	0.7628
AC	0.61	1	0.61	0.014	0.9087
BC	34.44	1	34.44	0.79	0.3955
Residual	437.07	10	43.71		
Lack of Fit	336.63	5	67.33	3.35	0.1052
Pure Error	100.43	5	20.09		
Corrected Total	1730.20	19			

Standard Deviation	6.61	R^2 = 0.7474
Mean	78.08	Adjusted R^2=0.5200
Coefficient of variation	8.47	Predicted R^2=-0.1791
Press	2040.06	Adequate R^2=6.420

3.7 Result and analysis

3.7.1 Tensile strength

The normal probability plot of the residuals for tensile strength shown in fig-8 reveals that the residuals are falling on almost the straight line, which means the errors are

distributed normally S Kumar [67]. All these consideration indicates an excellent adequacy of the quadratic model. Each observed value is compared with the predicted value calculated from the model in Figure.9

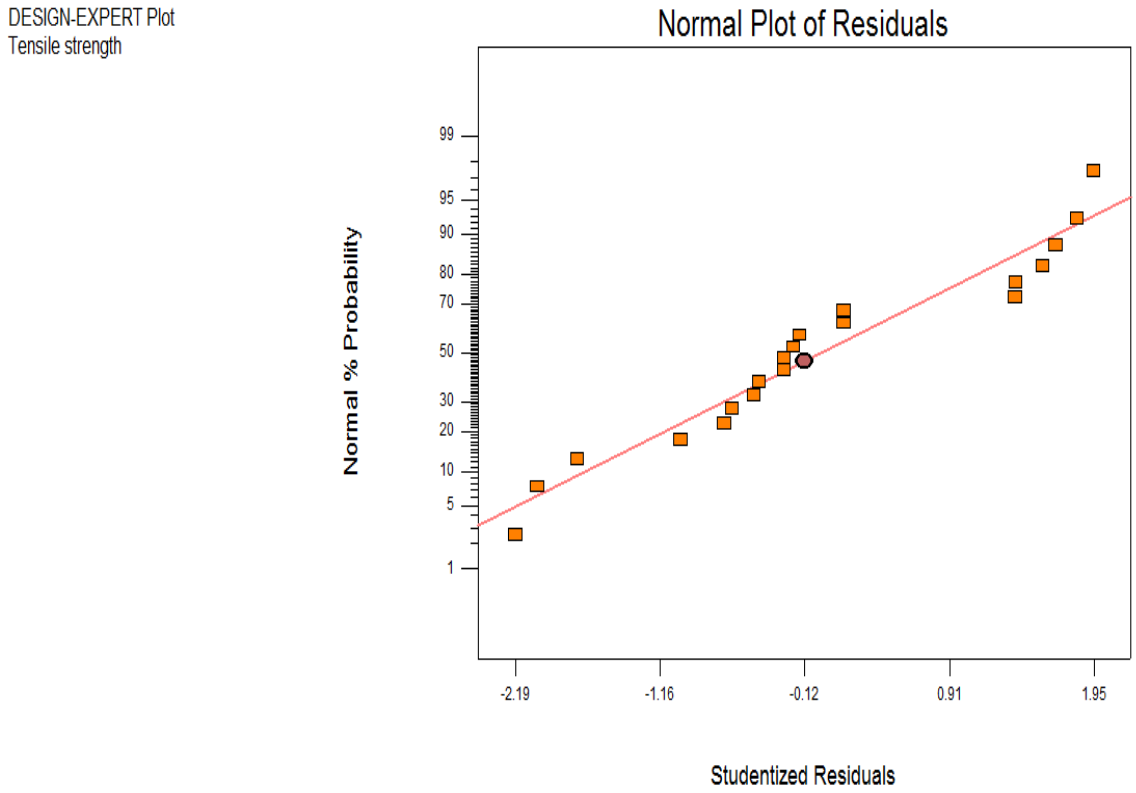

Figure 8-Normal probability plot of residuals for tensile strength

3.7.2 Optimising parameters

Contour graph show distinctive circular shape indicative of possible independence of factors with response. Contour graph is produced to visually display the region of optimal factor settings. For quadratic response surfaces, such a plot can be more complex than the simple series of parallel lines that can occur with first order models. First of all the stationary point is found, then it is usually necessary to characterize the response surface in the immediate nearby of the point. For this it is identified whether the stationary point found is a maximum response or minimum response or a saddle point. To analyse this, the simplest way is to examine through a contour graph. In the study of the response surface contour graph play a very important role. By generating contour plots using design expert software for response surface analysis, the optimum is located with reasonable accuracy by analysing the shape of the surface. If a contour patterning of circular shaped contours occurs, it tends to suggest independence of

factor. Response surfaces have been developed taking two parameters in the middle level and two parameters in the X and Y axis and response in Z axis. The response surfaces clearly reveal the optimal response point. RSM is used to find the optimal set of process parameters that produce a maximum or minimum value of the response.

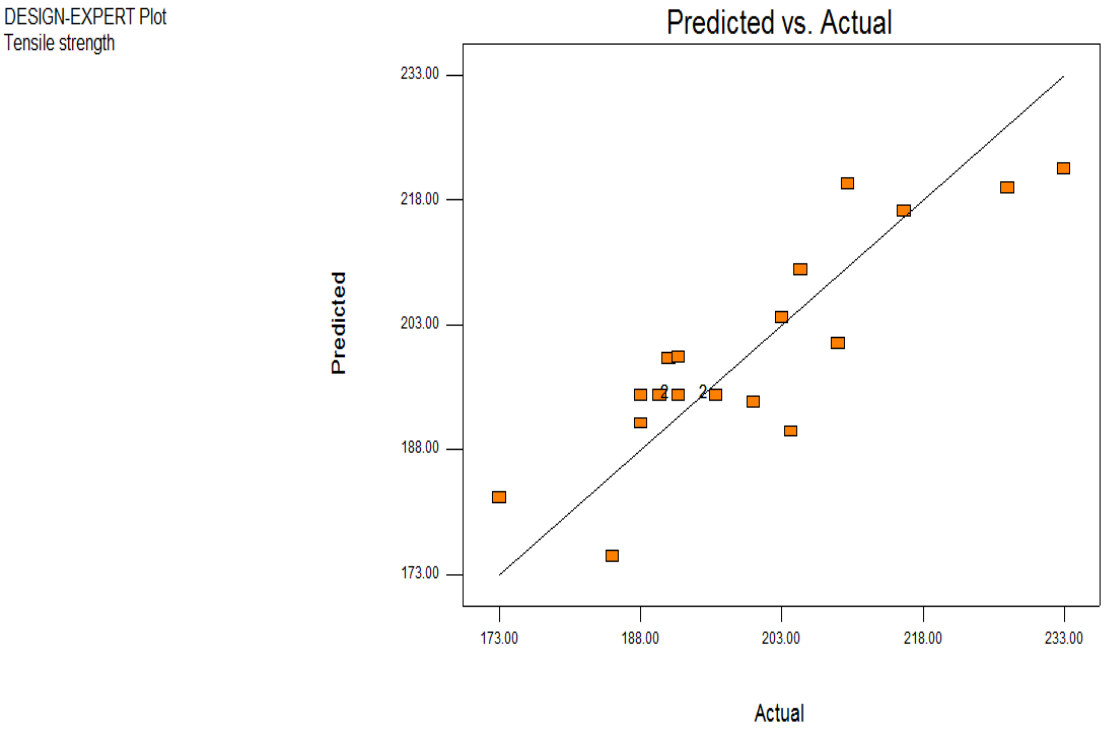

Figure 9- Actual vs predicted response of tensile strength

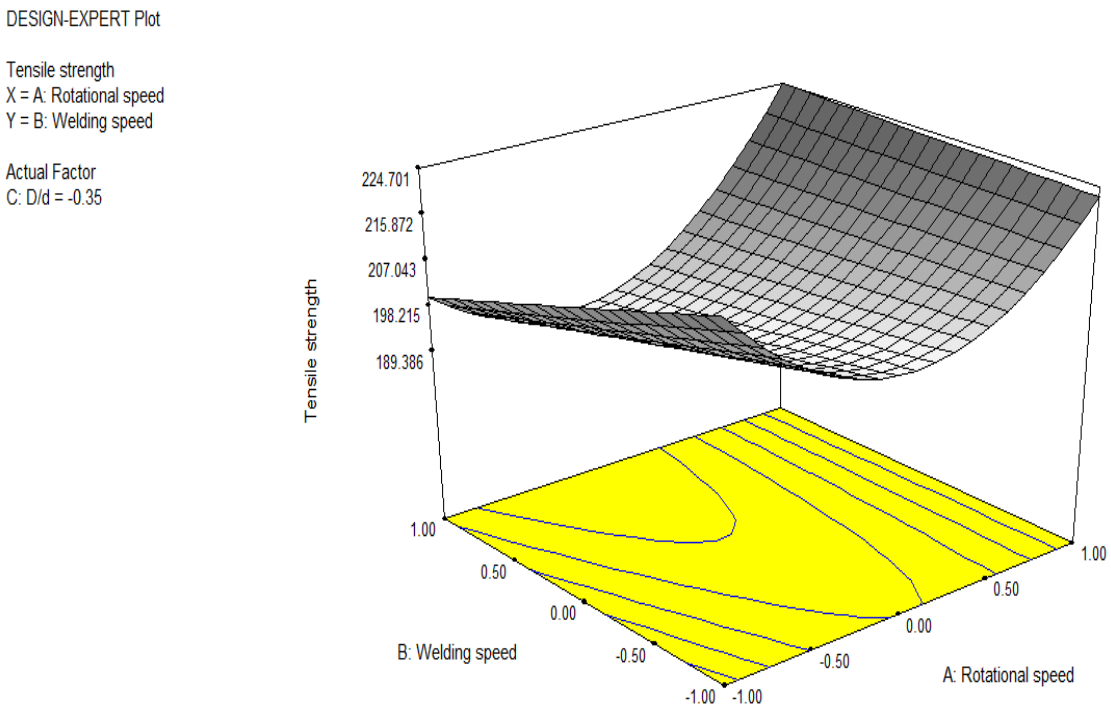

Figure 10-Tensile strength at const. D/d

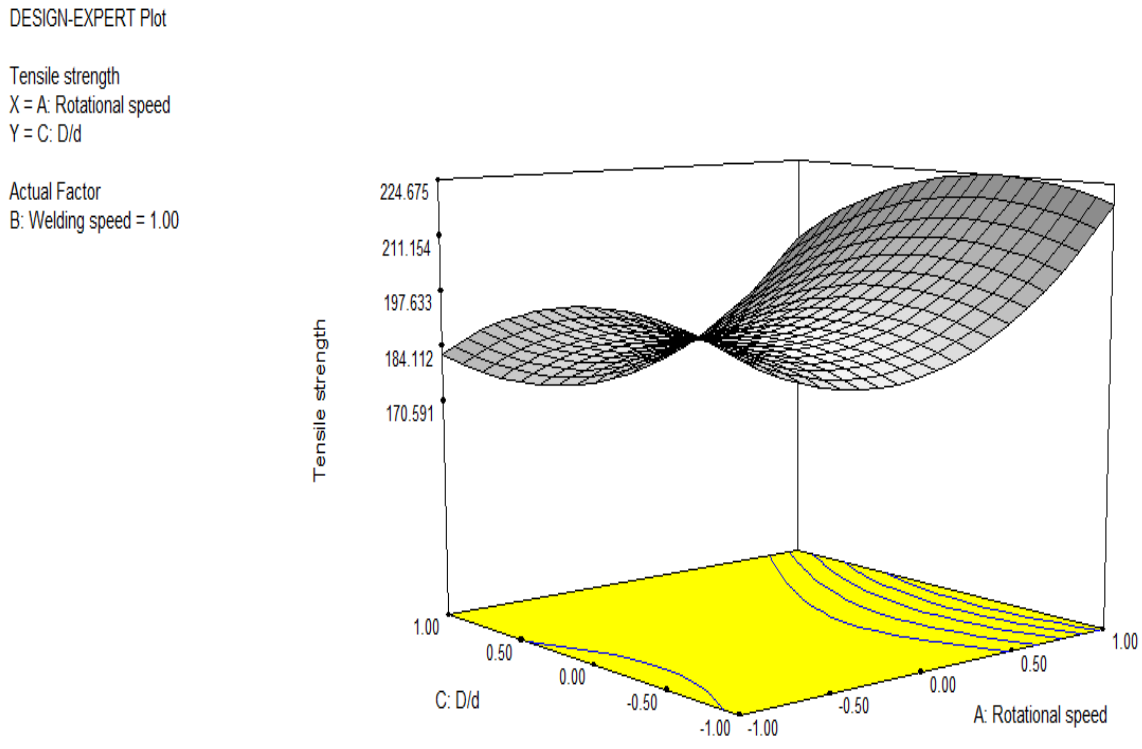

Figure 11-Tensile strength at const. welding speed

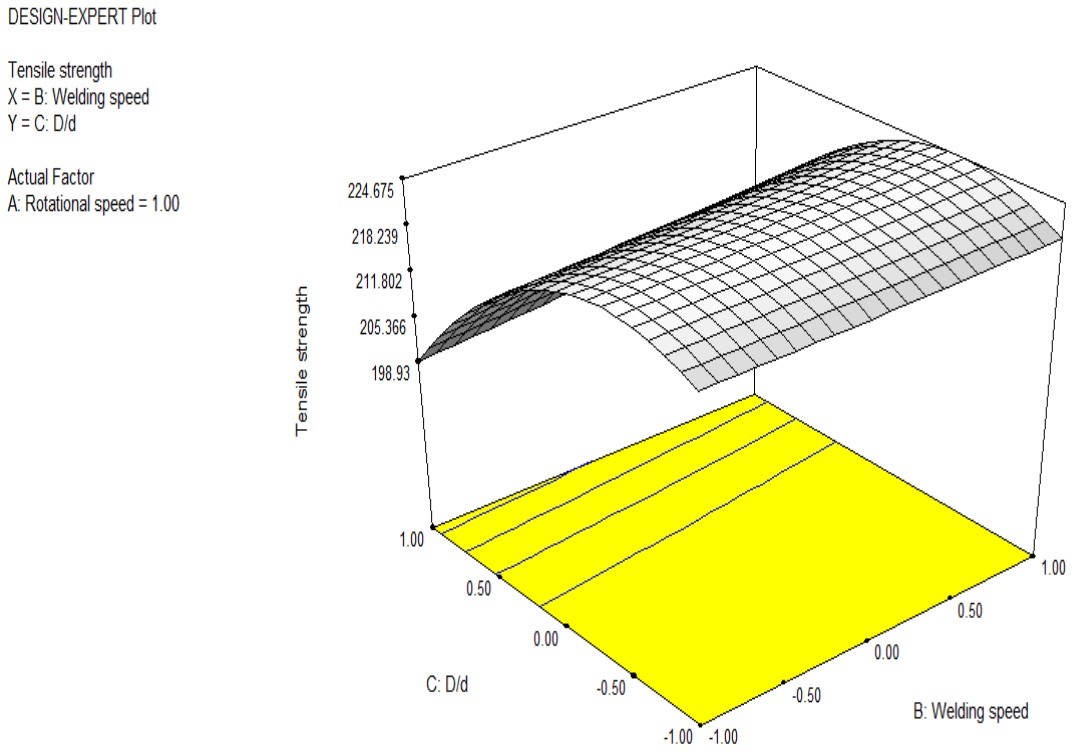

Figure 12-Tensile strength at const. rotational speed

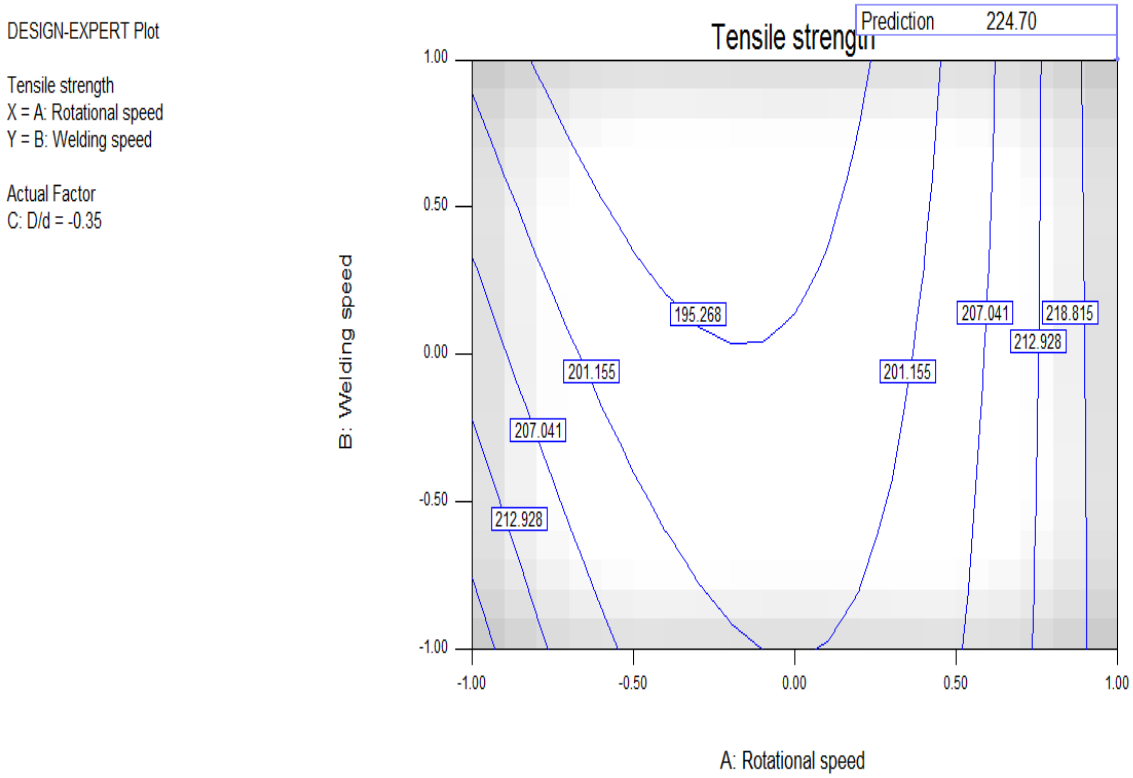

Figure 13-Contour of tensile strength at const. D/d

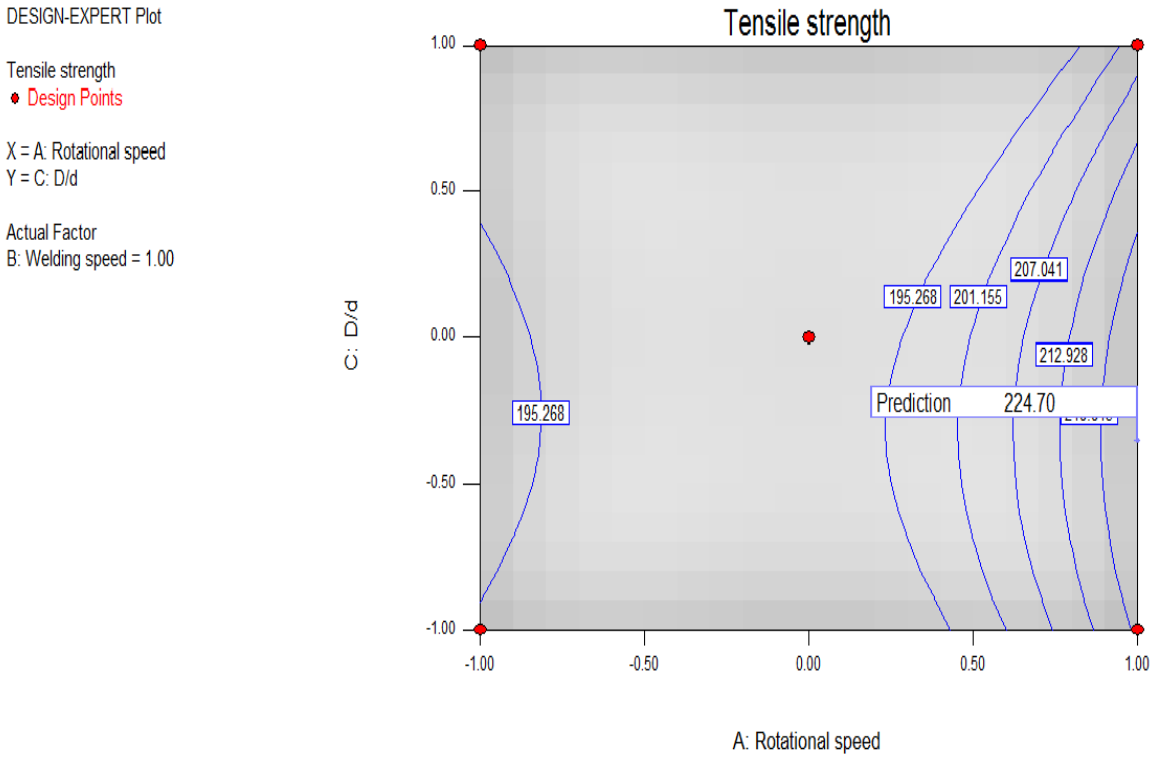

Figure 14-Contour of tensile strength at const. weling speed

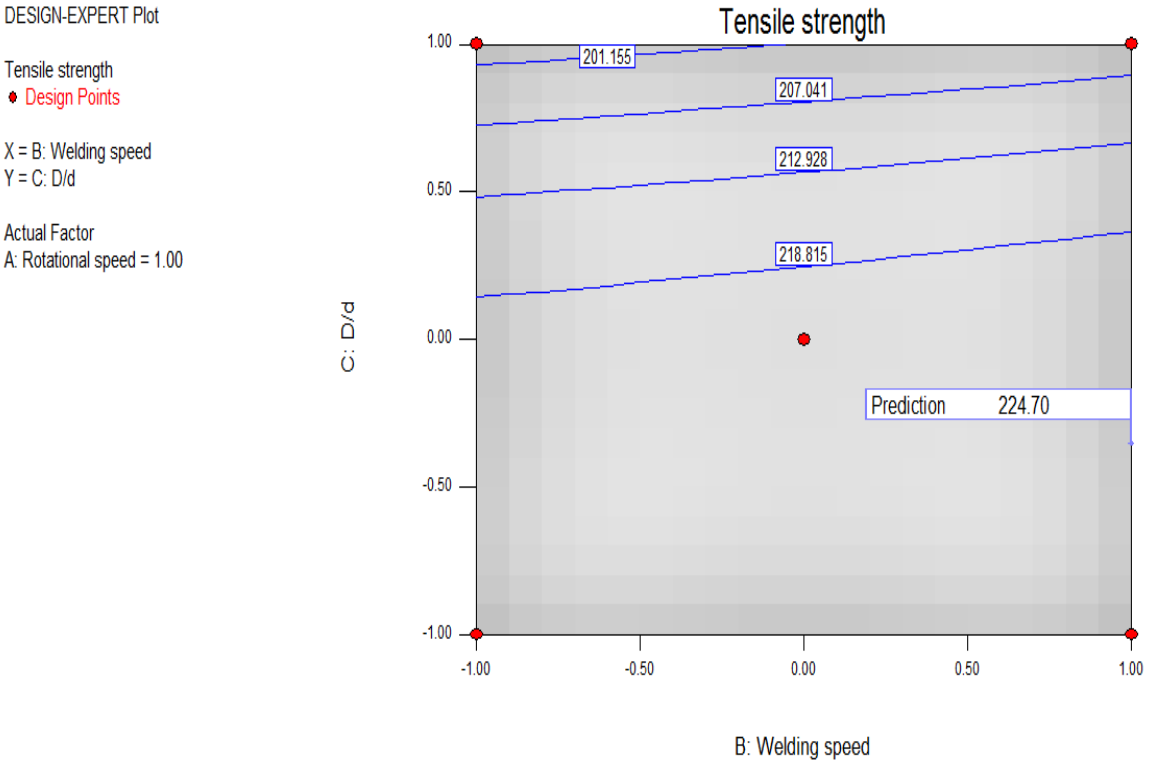

Figure 15-Contour of tensile strength at const. rotational speed

The present study the process parameters corresponding to the maximum tensile strength are considered as optimum (analyzing the contour graphs and by solving equation (4)). Hence, when these optimized process parameters are used, then it will be possible to attain the maximum tensile strength. Figure13-15 presents three dimensional response surface plots for the response tensile strength obtained from the quadratic model. The optimum tensile strength is exhibited by the apex of the response surface. Figure.14 exhibits almost a circular contour, which suggests independence of factor effect namely rotational speed. It is relatively easy by examining the contour plots (Figures.15 and 16), that changes in the tensile strength are more sensitive to changes in rotational speed than to changes in welding speed and shoulder diameter to pin diameter ratio. When welding speed is compared with D/d at a constant rotational speed of 1200 rpm, welding speed force is slightly more sensitive to changes in tensile strength as illustrated in contour plot (Figure16). Interaction effect between the factors rotational speed and welding speed, rotational speed and D/d, and welding speed and D/d on tensile strength also exists, which is evidenced from the contour plot. Increase in rotational speed resulted in drop in initial axial force with the interaction effect between rotational speed and welding speed, welding speed and D/d. Predicted optimum tensile strength obtained from the response surface and contour plots by using a rotational speed of 1200 rpm, welding speed of 90 mm/min, and D/d of 2.825 is 224.675 MPa.

3.7.3 Microhardness

The normal probability plot of the residuals for microhardness shown in figure 16 reveals that the residuals are falling on almost the straight line, which means the errors are distributed normally S Kumar [67]. All these consideration indicates an excellent adequacy of the quadratic model. Each observed value is compared with the predicted value calculated from the model in Figure17.

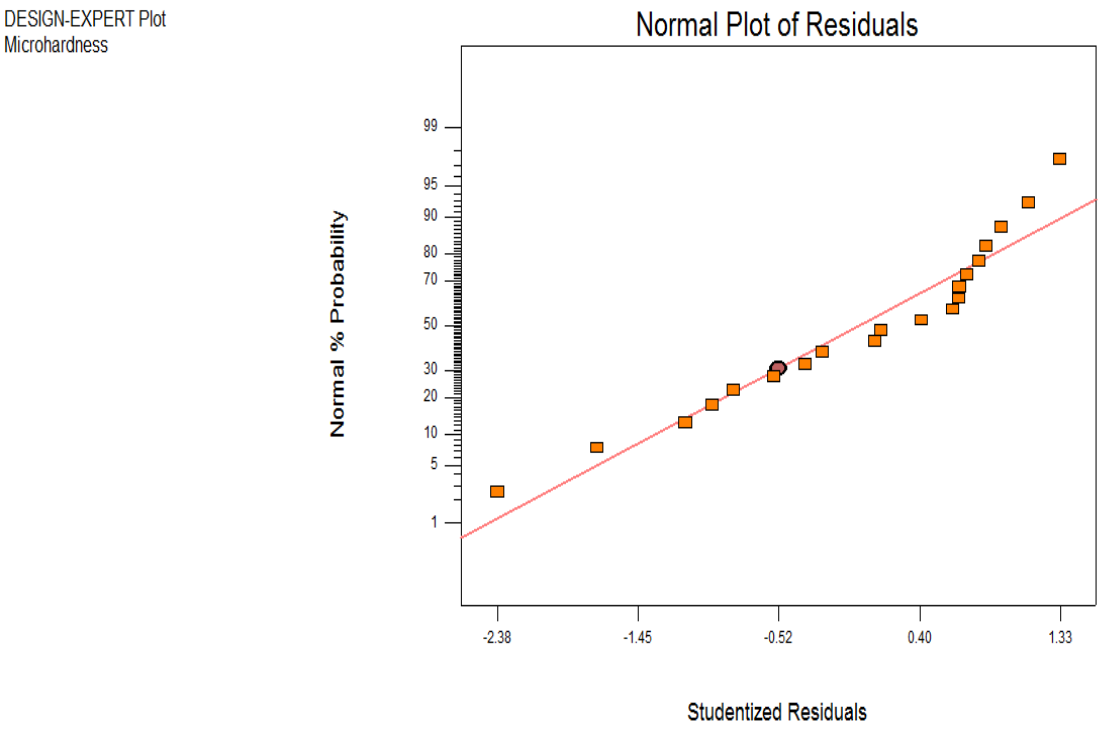

Figure 16- Normal plots of residuals for microhardness

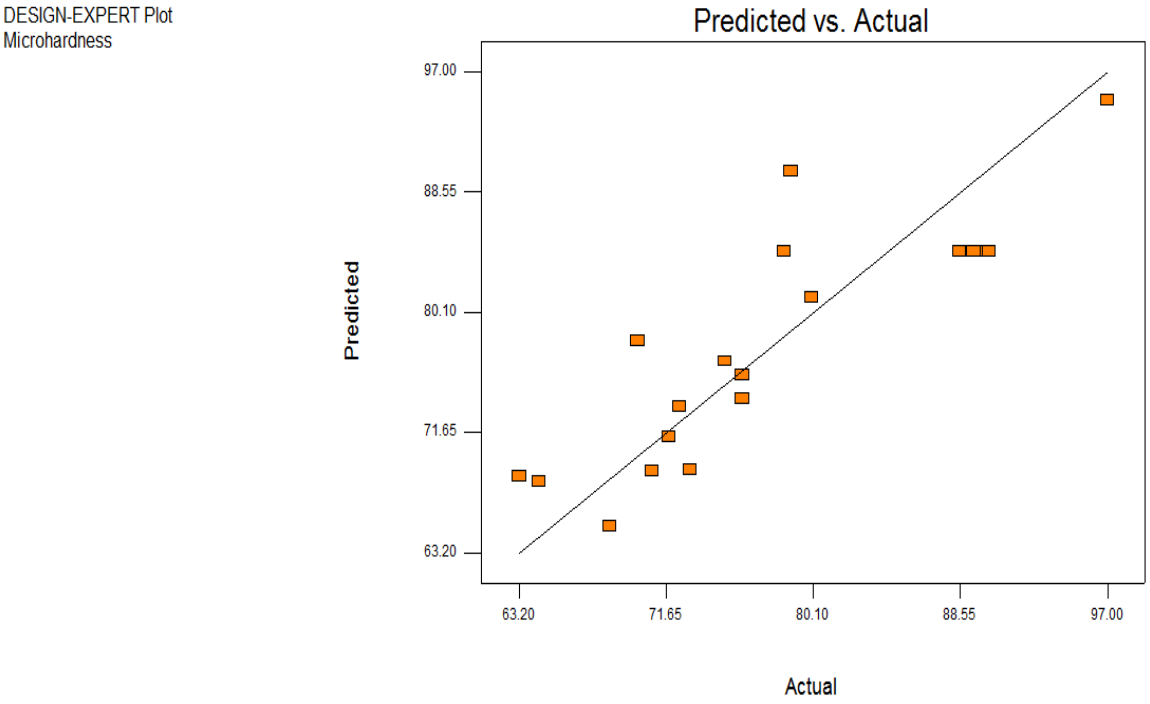

Figure 17-Predicted vs actual graph for microhardness

3.7.4 Optimizing Parameters

Contours graphs shows distinctive circular shape indicative of possible independence of factors with response. Contours graphs are produced to visually display the region of optimal factor settings. For quadratic response surfaces, such a plot can be more complex than the simple series of parallel lines that can occur with first order models. First of all the stationary point is found, then it is usually necessary to characterize the response surface in the immediate of the point. For this it is identified whether the stationary point found is a maximum response or minimum response or a saddle point. To analyse this, the simplest way is to examine through a contour graph. In the study of the response surface contour graph play a very important role. By generating contour plots using design expert software for response surface analysis, the optimum is located with reasonable accuracy by analysing the shape of the surface. If a contour patterning of circular shaped contours occurs, it tends to suggest independence of factor. Response surfaces have been developed taking two parameters in the middle level and two parameters in the X and Y axis and response in Z axis. The response surfaces clearly reveal the optimal response point. Response surface methodology (RSM) is used to find the optimal set of process parameters that produce a maximum or minimum value of the response. The present study the process parameters corresponding to the maximum microhardness are considered as optimum (analyzing the contour graphs and by solving Equation (5). Hence, when these optimized process parameters are used, then it will be possible to attain the maximum microhardness. Figure 18-20 presents three dimensional response surface plots for the response tensile strength obtained from the quadratic model.

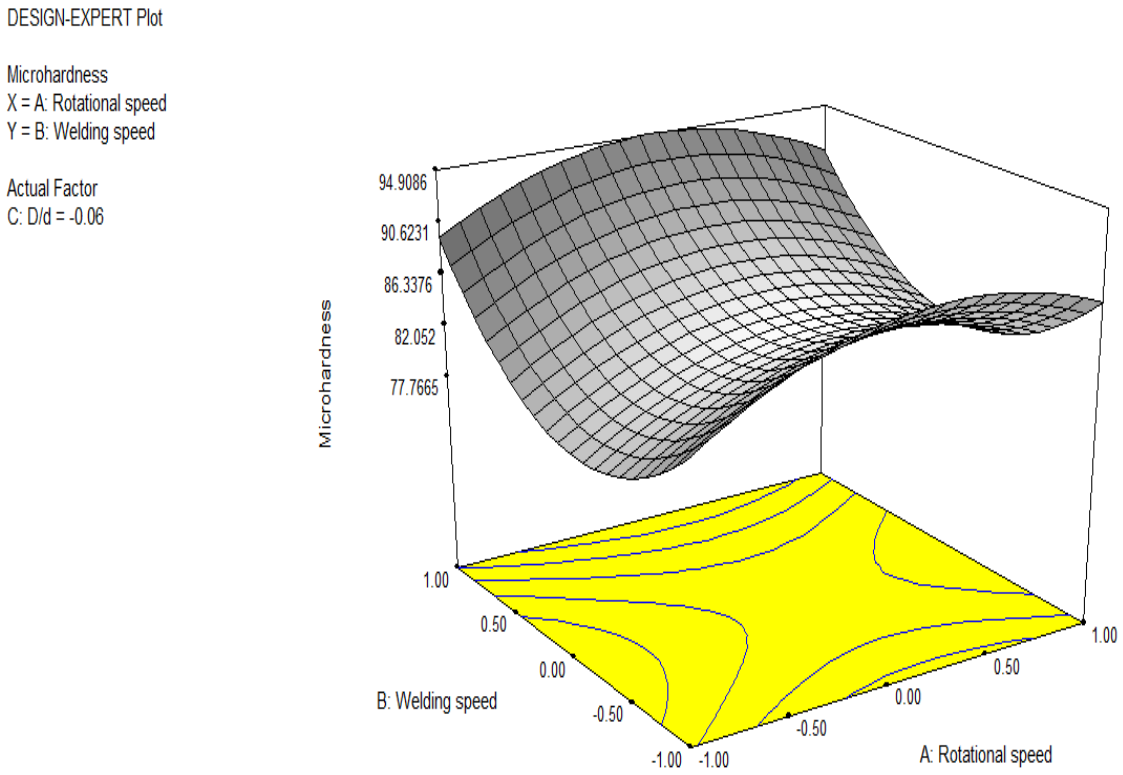

Figure 18-Microhardness at const. D/d

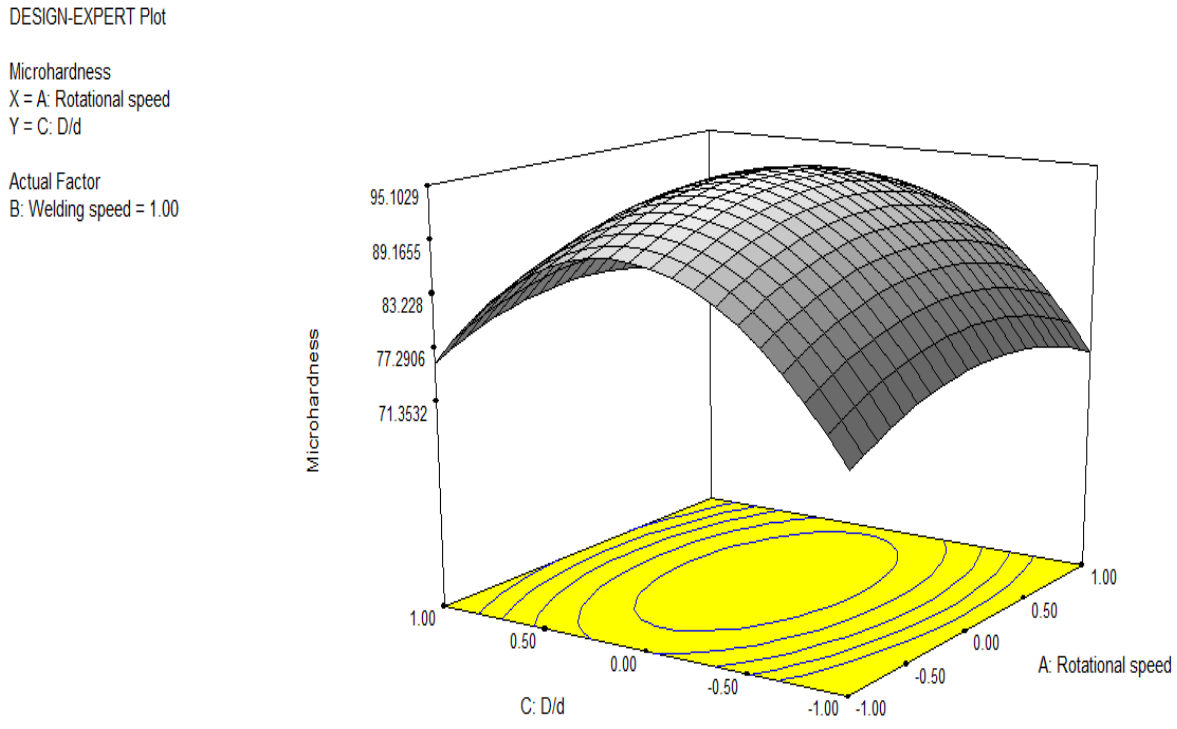

Figure 19-Microhardness at const. welding speed

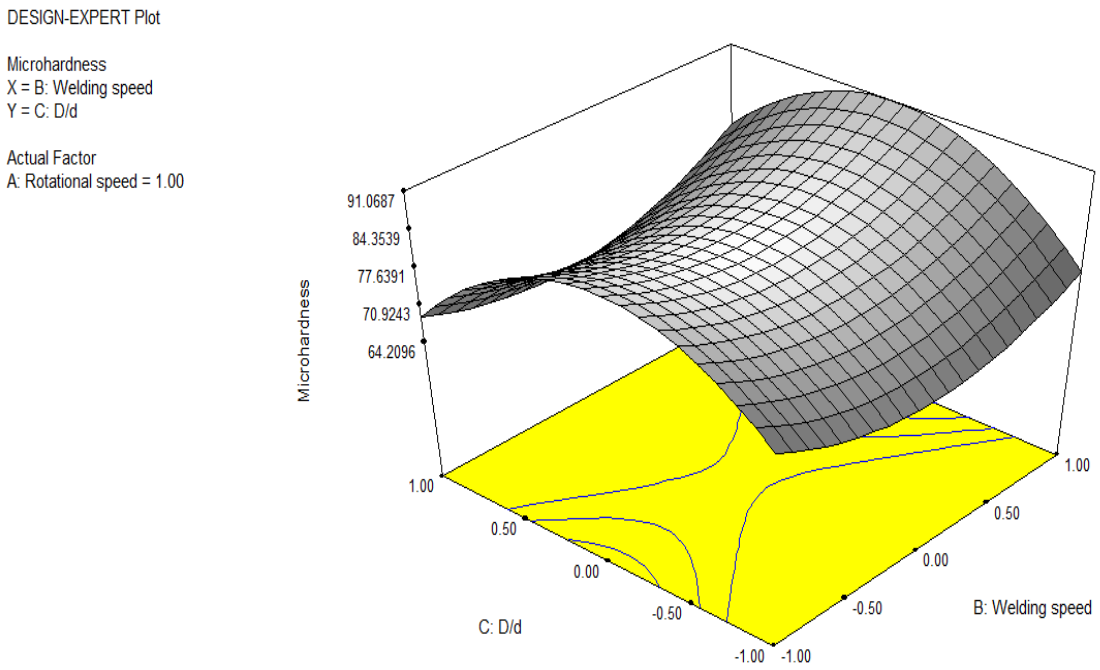

Figure 20-Microhardness at const. rotational speed

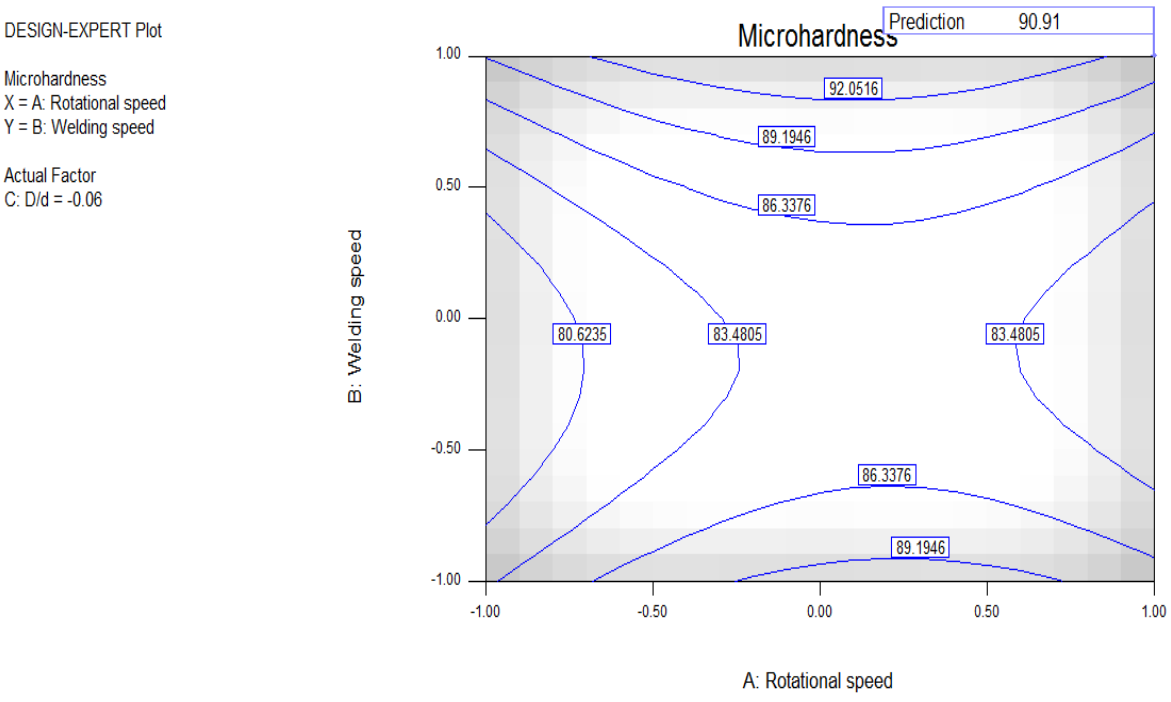

Figure 21-Contour of microhardness at const. D/d

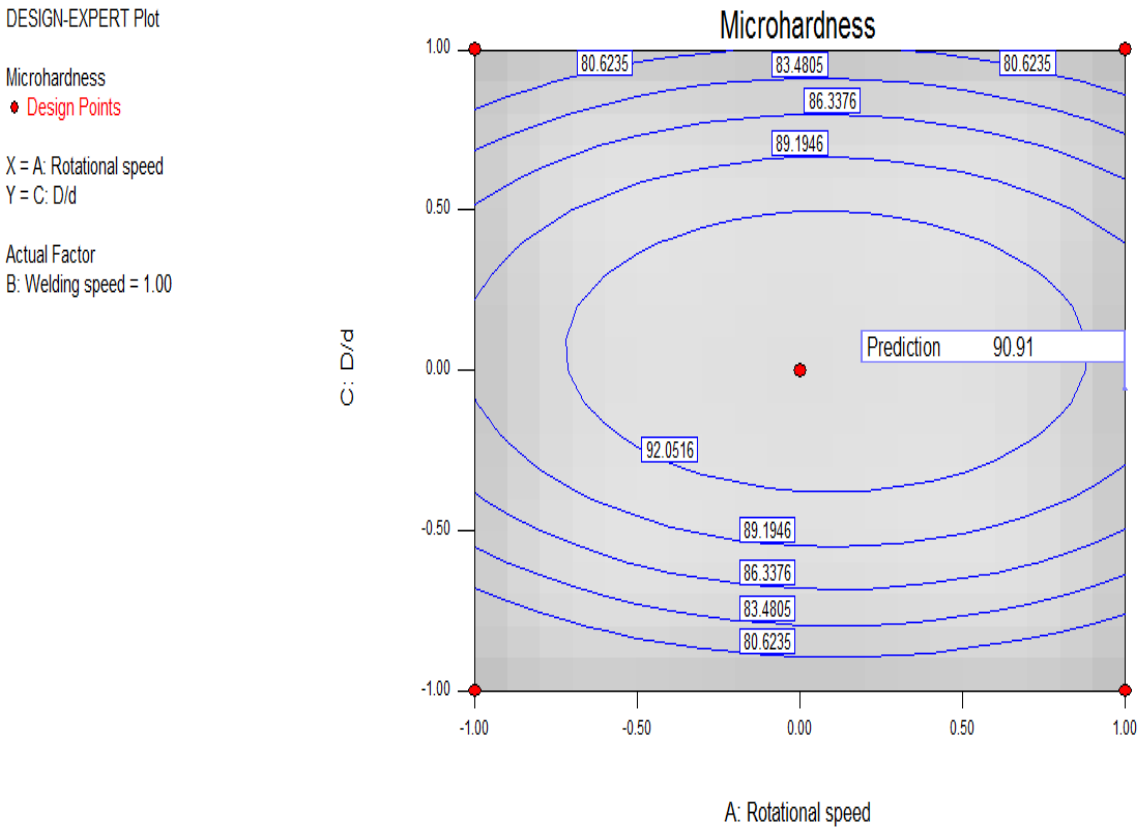

Figure 22-Contour of microhardness at const. welding speed

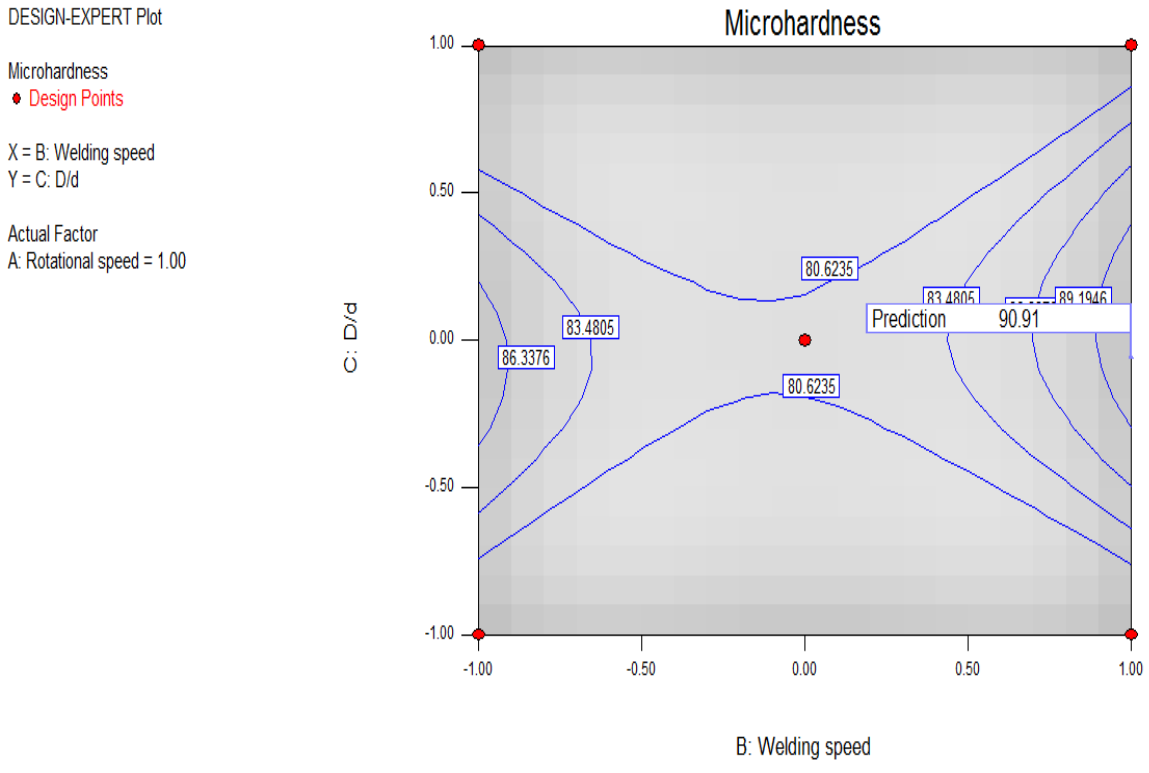

Figure 23-Contour of microhardness at const. rotational speed

The optimum microhardness is exhibited by the apex of the response surface. Figure 21 contour suggests dependence of factor effect namely rotational speed feed rate on microhardness is almost equal. Figure 22 is almost circular which shows independence of tool pin profile on micro hardness. The same is also depicted by Figure 23. When welding speed is compared with D/d at a constant rotational speed of 1200 rpm, welding speed force is slightly more sensitive to changes in microhardness as illustrated in contour plot Figure 23. Interaction effect between the factors rotational speed and welding speed, rotational speed and D/d, and welding speed and D/d on microhardness also exists, which is evidenced from the contour plot. Predicted optimum micro hardness obtained from the response surface and contour plots by using a rotational speed of 1200 rpm, welding speed of 90 mm/min, and D/d of 2.965 is 91.06 Hv.

CHAPTER-4

Experiment 2- Microstructural and mechanical behaviours of Nano-TiC-reinforced AA6082 FSW Joints at optimized parameters.

3.8 Introduction

After optimization of FSW parameters with response surface methodology it is evident that maximum tensile strength at given parameters can be 224.675 MPa. This is 74.4% of actual tensile strength (302 MPa) of base material. It means that strength of FSW joint decreases. The present work focuses on FSW of 6082 AA-T651 aluminium (Al) alloy which has gained wide acceptance in the fabrication of lightweight structures requiring higher strength, and excellent corrosion resistance. FSW of AA6082 was done with and without reinforcement of nano sized titanium carbide (TiC) particle of size 10-30 nm. The effect of processing parameters and reinforcement on the mechanical and microstructural properties of 6082 AA-T651 joints was analysed in this study. Welded specimens were produced by employing different combinations of feed rates (60 and 90 mm/min) and tool rotational speeds (1000 and 1200 rpm). Tensile test, microstructure, hardness and EDX (Energy dispersive X-ray spectroscopy) analysis has been performed to evaluate the weld zone molecular characteristics and strength of friction stir welded alloy. Result shows that welding process reduces the strength and hardness of material, which can be partially regained by reinforcement of TiC nano particles during welding process. Scanning electron microscope (SEM) equipped with EDX was used to analyse the chemical compositions of the alloy and titanium carbide particles of the weld nugget zone (NZ), which indicated that TiC is uniformly distributed in NZ.

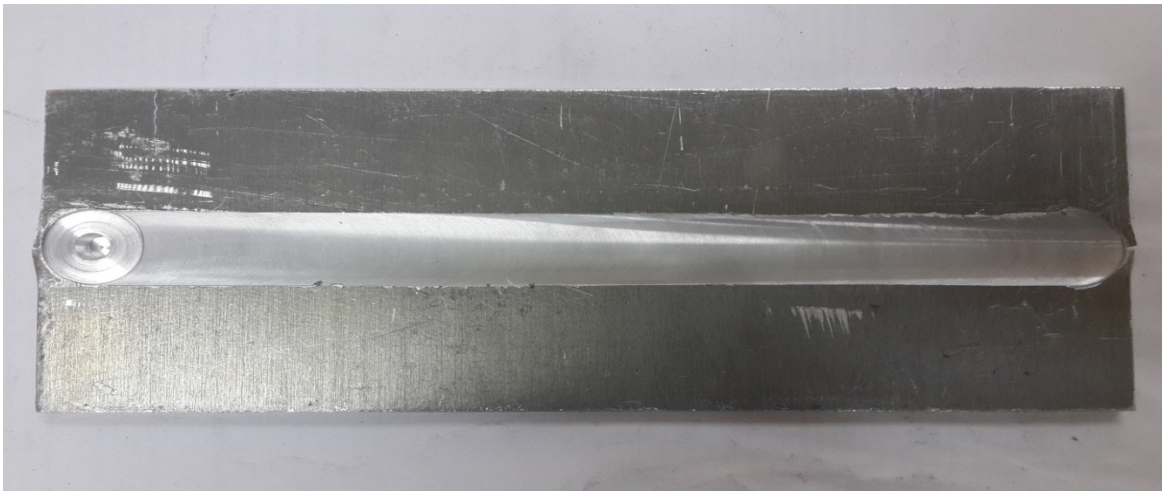

Figure 24-Friction stir welded AA6082 plate

3.9 Workpiece Material

A commercial 6082-T651 AA plate which is solution heat treated, stress relieved by stretching then artificially aged is used as specimen for FSW. Chemical composition of workpiece material is given in table 1.

3.10 Tool Used

A straight square tool pin is used for friction stir welding as shown in figure 25. It was fabricated from H13 hot working steel and heat treated to 58HRC (Hardness, Rockwell C-scale). This tool had a 5.7 mm long pin. The diagonal of square pin was 6 mm, Shoulder diameter of tool is18 mm.

Figure 25-Square shape pin tool

3.11 Experimental setup

An automatic friction stir welding machine (R V machine tools, FSW-4T-HYD) as shown in figure 4 is used for welding process. Other information about experimental setup is given in section 3.4

3.12 Experimental procedure

Plate of 6mm thickness, 80mm width and 200 mm length was prepared by machining through milling. Subsequently, a 0.6mm wide, 5mmdeep and adequately long profile was created on the faying surface of each plate. When two plates were fixed under a purpose-built fixture, asymmetrical bottom-closed groove was made lengthwise, shown in Figure 26. Next, the TiC nano particles were added into the groove and pressed tightly. Using threaded tapered pin with 2˚ tilt angle, FSW was carried out with and without TiC nano particles.

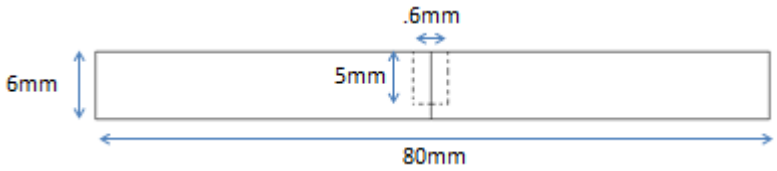

Figure 26- Cross section of plate to be welded

All the joints were produced with the following optimized welding speed and tool rotational speed.

Table 6-FSW parameters

	Specimen with reinforcement				Specimen without reinforcement	
	R_1 (1)	R_2 (2)	R_3 (3)	R_4 (4)	B_1 (5)	B_2 (6)
Tool rotational speed (rpm)	1200	1200	1000	1000	1200	1000
Welding speed (mm/min)	90	60	90	60	90	60

3.13 Testing

3.13.1 Tensile Test

Uniaxial tensile tests at room temperature were performed in order to evaluate the mechanical properties of the joints. To determine the tensile strength of the stir zone, small tensile test specimens were sectioned in transverse direction of the weld line with an electrical discharge machine (EDM). Specimen is cut as per ASTM:B557-06 standard which is shown in figure.6. Tensile test is performed at a speed of 1mm/min.

Figure 27-Tensile test Machine

Figure 28- Tensile test specimen before and after the test

3.13.2 Micro hardness Test

Vickers hardness of friction stir welded AA6082 samples were measured using Vickers hardness tester. The test load applied was 200 gf and the dwell time was 5 seconds. Various samples FS welded at different rotational and translational speed were tested and also different longitudinal positions were also tested. The averages of five values of hardness within each tested area were considered. All samples were taken from the transverse section of the welded area at the middle of the sheet thickness; the same as the samples for microstructural investigation.

3.13.3 Microstructural analysis

Optical microscope was used to investigate the microstructure of a material. Samples for microstructural investigation were cut from the FSW zone in a transverse direction with respect to the welding line. The sample preparation for the microscopic investigation includes grinding, dry and wet polishing with Al_2O_3 nano powder. After polishing Keller's etchant is applied on surface to reveal the grain boundary and micro structure of welded zone. It gives the clear view of different microstructural zone like stir zone (SZ), heat affected zone (HAZ), thermo mechanical affected zone (TMAZ). It also revealed the distribution of TiC nano partical in stir zone.

3.13.4 SEM (scanning electron microscopy)

Scanning electron microscopy (SEM) is used to investigate the microstructural modifications induced by the FSW process on the aluminium alloy matrix and reinforcement particles. Samples for microstructural investigation were cut from the

base material and FSW zone in a transverse direction with respect to the welding line. It is known that a homogeneous distribution of the reinforcement particles is one of the main requirements to achieve good mechanical properties in discontinuously reinforced composites.

Figure 29-SEM setup

3.13.5 EDX (energy dispersive X-ray spectroscopy)

The chemical compositions of the matrix and titanium carbide particles of the weld nugget were analysed by a scanning electron microscope equipped with an energy dispersive X-ray spectroscopy (EDX) analysis system. The specimens were polished using conventional polishing methods and etched before analysis.

3.14 Result and discussion

Study on FSW of 6082-T6 with processing parameters ranging from 1000 to1200 rpm and 60 and 90 mm/min is conducted. Tensile test result shows that, tensile strength of Friction stir joint decreases with respect to the base material. Ehab A. El-Danaf et al [46] also reported this phenomenon of ,softening in the stir zone(SZ) and thermo mechanical affected zone (TMAZ) in Friction stir welding of AA 6082 - T651.when welding is done at Response surface methodology (RSM) optimized parameters tensile strength is achieved 234 MPa, which is 77.5% of tensile strength

(302 MPa) of base alloy. To avoid the softening of stir zone or reduction of tensile strength TiC nano particles is added during Friction stir welding. Tensile test results clearly shows that inclusition of TiC partical partially amended the strength loss that occurred with FSW. The average SZ hardness, the yield and tensile strength have increased after TiC nano partical inclusion during Friction stir welding. Tensile strength of different F S Welded specimen is given in figure 30.

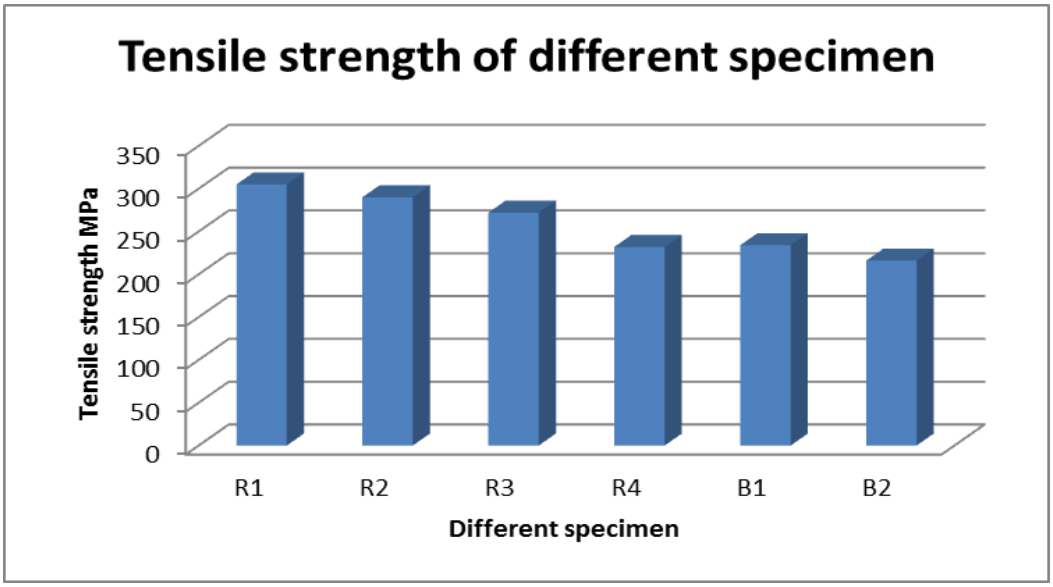

Figure 30 -Tensile strength of different specimen

Microhardness values of friction stir welded AA 6082 alloy and FS welded AA6082 with Tic nano particles at 1200 rpm, 90 mm/min is shown in figure 31. Joint obtained at optimized parameters shows that softening occurs in the stir zone (SZ) and thermo mechanical affected zone (TMAZ) compared to the unaffected base. The softening with respect to the base metal is due to the decomposition of needle-shaped β" precipitates which is the main source of hardening and strengthening, the coarsening of precipitates into semi- and non-coherent rod-shaped β' precipitates (over-aged precipitate structure) and the low dislocation density associated with the dynamically recrystallized structure [68]. Another probable reason is that intense deformation causes fragmentation of second phase particles and precipitates leading them to be redistributed in new locations at the interior of grains as reported by Dadbakhsh et al. [69]. This consequently leads to less strain and stress localization contributing to material softening. The TMAZ exhibited significant softening when

compared with the SZ. This has been noted on both the advancing and retreating sides as shown in Figure 29.

TiC nano particles are induced during welding to increase the strength and hardness of joint. The microstructural changes induced by the reinforcement of TiC particles are responsible for the improvement in mechanical properties. The possible strengthening mechanisms are discussed subsequently. TiC particles are dispersed over the entire aluminium matrix which provides Orowan strengthening [70]. The movement of dislocation encounters resistance owing to the presence of TiC particles in the AMCs and the path of dislocation movement is diverted. The dislocation density of the AA6082/TiC AMC is relatively higher compared to unreinforced matrix alloy. The thermal mismatch and differential deformation creates additional dislocations in the AMC. The increased dislocation density rises to the resistance to the motion of dislocation across the material. The excellent interfacial bonding between the aluminium matrix and the TiC particle brings the load transferring mechanism into operation. The effective transfer of load from the aluminium matrix to the TiC particles strengthens the AMC joint.

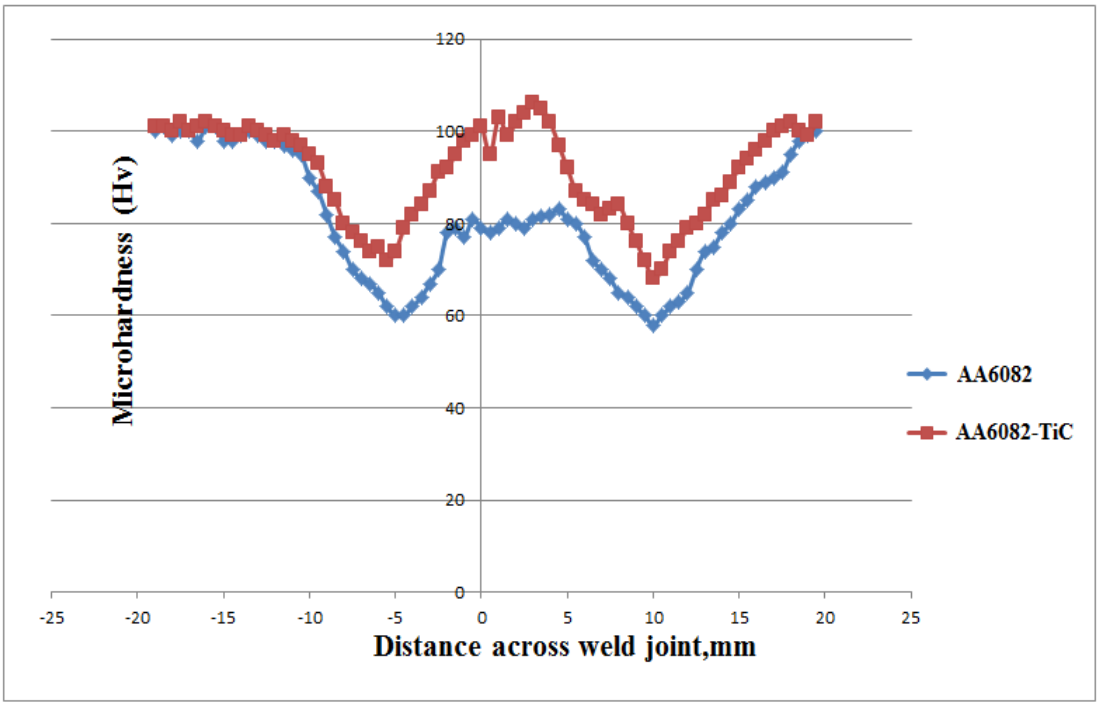

Figure 31- Micro hardness value of different specimen

Figure 32 shows the microstructure of AA 6082 –TiC composite, it indicates the homogenous distribution of TiC particles in stir zone (SZ) Optical micrographs in

Figure 32 show the typical zones of the weld nugget or stirred zone (SZ), the transitional zone (TZ) and the base material (BM). The transitional zones in FSW unreinforced aluminium alloys generally consisted of the thermomechanical affected zone (TMAZ) and heat-affected zone (HAZ), but probably due to the well-known lower sensitivity to thermal variations of ceramic reinforced composites, it was difficult to identify the HAZ, as also reported by Amirizad et al. [71]. The welded zone was mainly identified by a different size of the reinforcement particles a d the aluminium alloy matrix with respect to the base material.

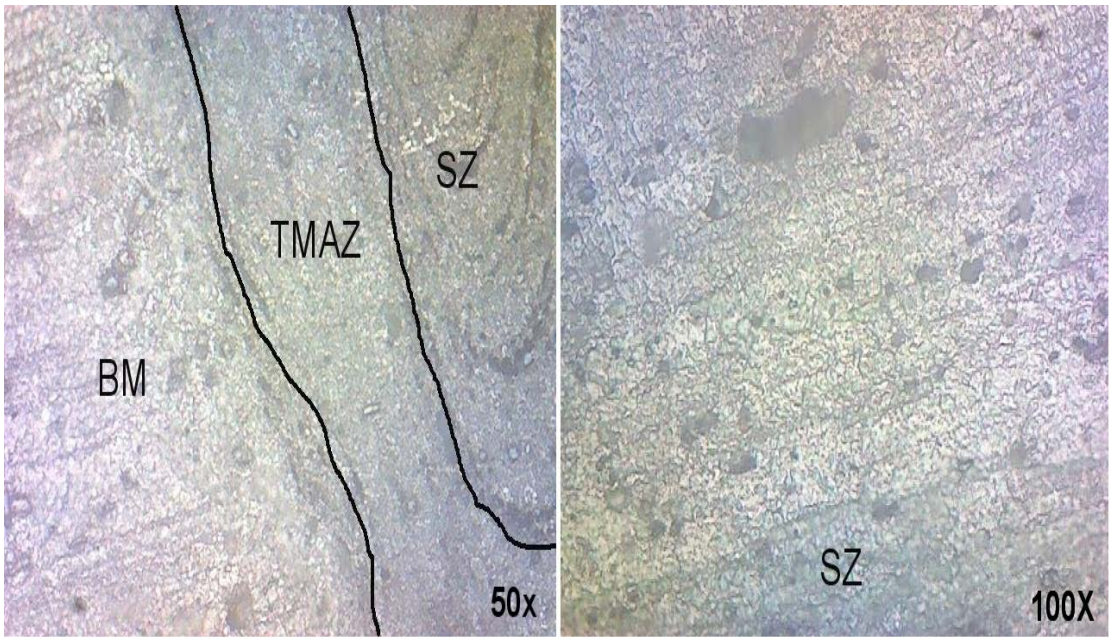

Figure 32-Micro structure of FSW AA 6082 -TiC alloy

The SEM micrographs of the friction stir welded specimen are shown in Figure 33. The distribution of TiC particles is fairly homogeneous in the stir zone. During the initial stages of the formation of the joint, the plasticized aluminium alloy flows into the groove and forged at the back of the tool. The rotating action of the tool provides a vigorous stirring which causes the packed TiC particles in the groove to be uniformly distributed in the aluminium matrix. Since the joint is formed in the solid state, the free movement of particles due to density gradient is absent. However, an agglomeration of TiC particles was observed at few places. The light regions in the macrostructure (Figure 33) exhibit bands of TiC particles. Those regions were present close to the centre of the joint. The grains are not clearly visible in Figure 33 because they are ultrafine in nature. The grain modification can be attributed to the presence of TiC particles in the joint because TiC particle acted as an effective grain

refiner. The stirring action of the tool and the intense plastic strain were known to break the ceramic particles TiC particles retained the original size and morphology which can be attributed to their initial smaller size. This result agrees with the findings of Chen et al. [72] who did not observe fragmentation of B_4C particles in FSWof AA6063/ B4C AMC due to its smaller size.

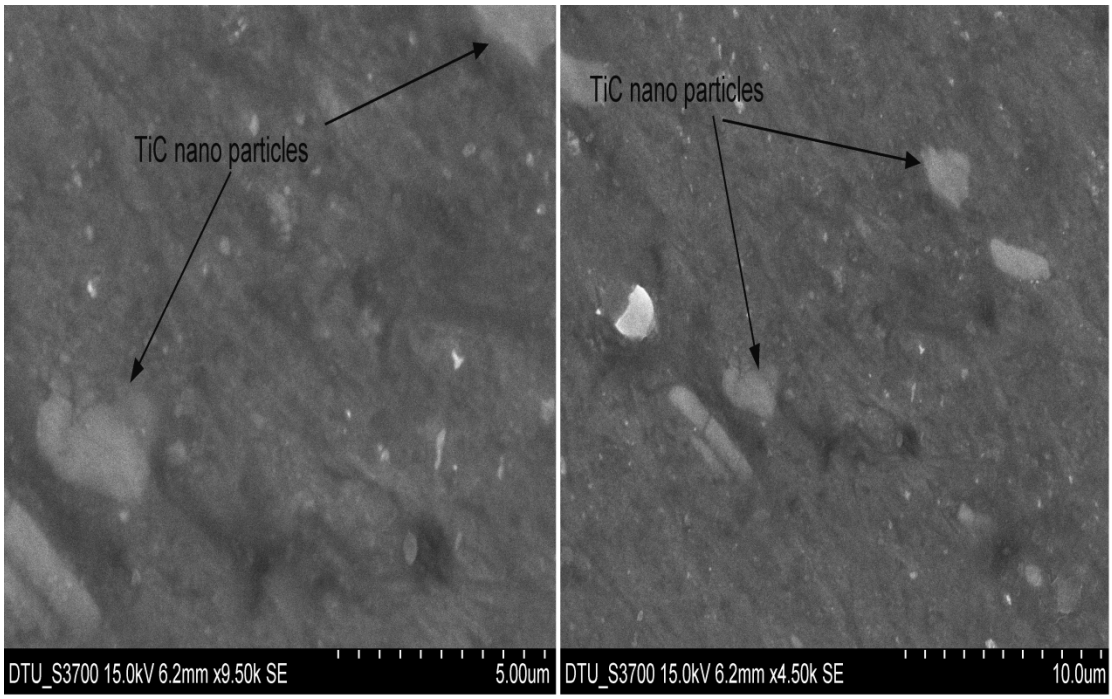

Figure 33 SEM micro graph of FSW AA66082-TiC joint

Fatigue behaviour of specimen can be obtained from an analysis of the fracture behaviour. For the friction stir welded specimens failure occurred in the middle line of the stirred zone .SEM analyses of the fracture surfaces showed, the lack of penetration in the joint,

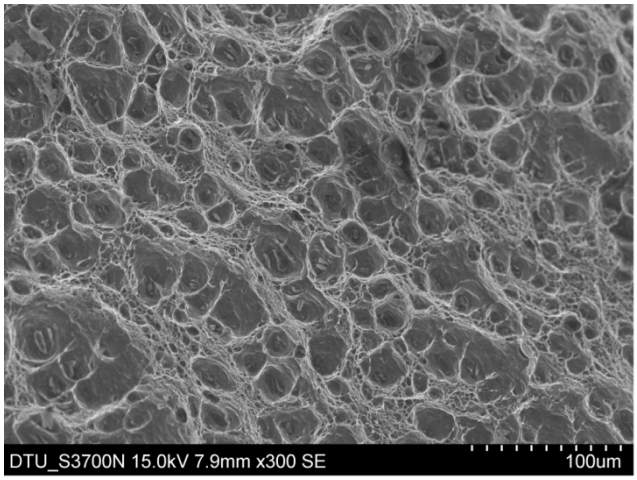

Figure 34-SEM micrograph of fracture surface of FSW AA6082-TiC alloy

For this specimen, since failure occurred in the stirred zone, very fine reinforcement particles were visible in the fracture surface, together with fine dimples due to the ductile fracture of the aluminium alloy matrix (Figure. 34)

The chemical compositions of the matrix and titanium carbide particles of the weld nugget were analysed by a scanning electron microscope equipped with an energy dispersive X-ray spectroscopy (EDX) analysis system. This analysis indicates that distribution of TiC particles is uniform in weld nugget zone.

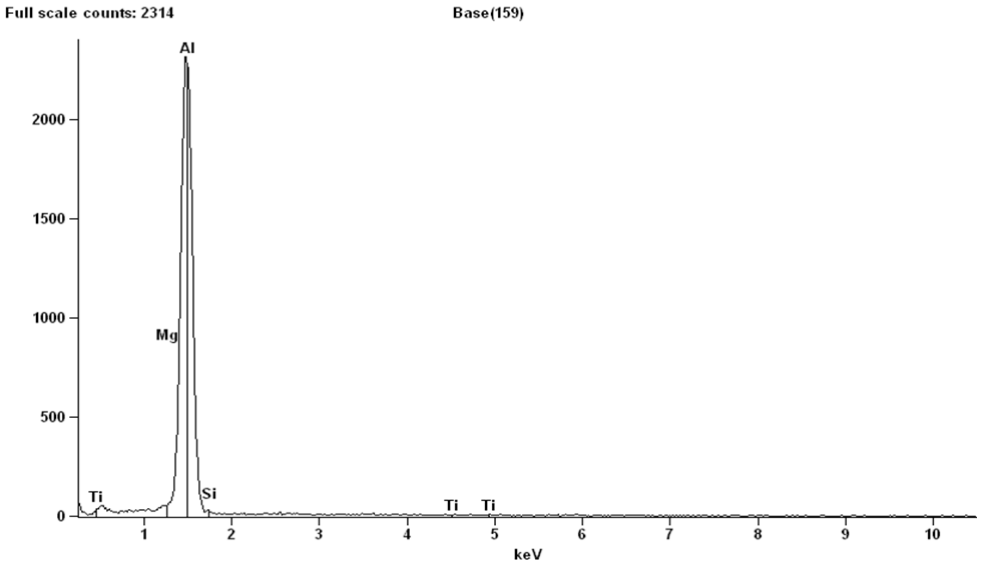

Figure 35-EDX analysis graph

Conclusions

An AA6082–T651 alloy was friction stir welded, using different welding parameters, and the effects of this process on microstructure, tensile and microhardness were investigated.

1. The central composite face centred designed experiments of FSW on design expert were successfully conducted and the process parameters have a critical role in the quality of the obtained composites.
2. Rotational speed is the factor that has greater influence on tensile strength, followed by welding speed and Shoulder diameter to pin diameter ratio.
3. The FSW process parameters were optimized to maximize the tensile strength, the optimum condition of rotational speed, welding speed, and Shoulder diameter to pin diameter ratio (D/d) were found to be 1200 rpm,.90 mm/min and 2.825 respectively.
4. The FSW process parameters were optimized to maximize the microhardness, the optimum condition of rotational speed, welding speed, and Shoulder diameter to pin diameter ratio (D/d) were found to be 1200 rpm, 90 mm/min, and 2.965.
5. Tensile properties at optimum condition were lower in small quantity as compare to the parent material due to presence of reinforcement particles which make the metal matrix brittle.
6. Micro hardness at optimum condition was higher in small quantity as compare to the parent material due to grain refinement.
7. Welding of AA6082 results in softening in the SZ and TMAZ being more significant. This negative effect on the welded joints strength and hardness can be partially recovered by inclusion of TiC nano particles during welding.
8. Microstructural and SEM analysis clearly indicate that distribution of TiC nano particles is homogenous in Stir zone (SZ).

References

[1] Root J.M., Field D.P., Nelson T.W., Crystallographic texture in the friction-stir welded metal matrix composite Al6061 with 10 Vol % Al_2O_3, Metallurgical and Materials Transactions A, 40(A) (2009) 2109–14.

[2] Chidambaram A., Bhole S.D., Metallographic preparation of aluminum–alumina metal matrix composites, Materials characterization, 38 (3) (1997) 187–91.

[3] Key property data for AMC's products. Available from: www.amcmmc. co.uk.

[4] Storjohann D., Babu S.S., David S.A., Sklad P., Report on U.S. Department of Energy, Office of Heavy Vehicle Technology and Office of Transportation under contract number DE-ACO5- 000R22725 with UT-Battelle LLC, 2002, 1–4.

[5] Clyne T.W., Withers P.J., An introduction to metal matrix composites, Cambridge University Press, 1993.

[6] Lean P.P., Gil L., Urefia A., Dissimilar welds between unreinforced AA6082 and AA6092/SiC/25p composite by pulsed-MIG arc welding using unreinforced filler alloys (Al–5Mg and Al–5Si), Journal of Materials Processing Technology, 143–144 (2003) 846–50.

[7] Spowart J.E., Ma Zong-Yi, Mishra R.S., The effect of friction stir processing (FSP) on the spatial heterogeneity of discontinuously reinforced aluminum (DRA) microstructures, Friction stir welding and processing II, TMS Publication. 243–52.

[8] Wert J.A., Microstructures of friction stir weld joints between an aluminium base metal matrix composite and a monolithic aluminium alloy, Scripta Materialia, 49 (2003) 607–12.

[9] Femandez G.J., Murr L.E., Characterization of tool wear and weld optimization in the friction-stir welding of cast aluminium 359 + 20% SiC metal–matrix composite, Materials Characterization, 52 (2004) 65–75.

[10] Nakata K., Inoki S., Nagano Y., Ushio M., Friction stir welding of Al_2O_3 particulate 6061 Al alloy composite, Material Sciemce Forum, 426-432 (2003) 2873–8.

[11] Gibsona B.T., Lammlein D.H., Prater T.J., Longhurst W.R., Cox C.D., Ballun M.C., Dharmaraj K.J., Cook G.E., Strauss A.M., Friction stir welding: Process, automation, and control, Journal of Manufacturing Processes, 16 (2014) 56–73.

[12] El-Danaf E.A., El-Rayes M. M., Microstructure and mechanical properties of friction stir welded 6082 AA in as welded and post weld heat treated conditions, Materials and Design, 46 (2013) 561–572.

[13] Ericsson M., Sandstrom R., Influence of welding speed on the fatigue of friction stir welds, and comparison with MIG and TIG, International Journal of Fatigue, 25 (2003) 1379–87.

[14] Simar A., Bréchet Y., Meester B., Denquin A., Gallais C., Pardoen T., Integrated modeling of friction stir welding of 6xxx series Al alloys: Process, microstructure and properties, Progress in Materials Science, 57 (2012) 95–183.

[15] Koumoulos E.P., Charitidis C.A., Daniolos N.M., Pantelis D.I., Nanomechanical properties of friction stir welded AA6082-T6 aluminum alloy, Materials Science and Engineering B, 176 (2011) 1585– 1589.

[16] Scialpi A., Filippis L.A.C., Cavaliere P., Influence of shoulder geometry on microstructure and mechanical properties of friction stir welded 6082 aluminium alloy, Materials and Design, 28 (2007) 1124–29.

[17] Cavaliere P., De Santis A., Panella F., Squillace A., Effect of welding parameters on mechanical and microstructural properties of dissimilar AA6082–AA2024 joints produced by friction stir welding, Materials and Design 30 (2009) 609–16.

[18] Liu H.J., Hou J.C., Guo H., Effect of welding speed on microstructure and mechanical properties of self-reacting friction stir welded 6061-T6 aluminum alloy, Materials and Design 50 (2013) 872–78.

[19] Jata K.V., Semiatin S.L., Continuous dynamic recrystallization during friction stir welding, Scripta Materialia, 43 (2000) 743–48.

[20] Nandan R., Roy G.G., Lienert T.J., Deb Roy T., Numerical modelling of 3D plastic flow and heat transfer during friction stir welding of stainless steel, Science and Technology of Welding and Joining, 11 (2006) 526–37.

[21] Nandan R., Roy G.G., Lienert T.J., Deb Roy T., Three-dimensional heat and material flow during friction stir welding of mild steel, Acta Materialia, 55 (2007) 883–95.

[22] Nandan R., Lienert T.J., Deb Roy T., Toward reliable calculations of heat and plastic flow during friction stir welding of Ti– 6Al–4V alloy, International Journal of Materials Research, 99 (2008) 434–44.

[23] Khandkar M.Z.H., Khan J.A., Reynolds A.P., Prediction of temperature distribution and thermal history during friction stir welding: input torque based model, Science and Technology of Welding and Joining, 8 (2003) 165–74.

[24] Bhadeshia H.K.D.H., Mathematical models in materials science, Material Science Technology, 24 (2008) 128–35.

[25] Arbegast W.J., Jin Z., Beaudoin A., Bieler T.A., Radhakrishnan B., Hot Deformation of Aluminum Alloys III, TMS, Warrendale, PA, USA, 2003, page. 313.

[26] Arbegast W.J., Jin Z., Beaudoin A., Bieler T.A., Radhakrishnan B., Hot Deformation of Aluminum Alloys III, TMS, Warrendale, PA, USA, 2003, p. 313.

[27] Thomas W.M., Johnson K.I., Wiesner C.S., Friction stir welding-recent developments in tool and process technologies, Advanced Engineering Material, 5 (2003) 485–90.

[28] Thomas W.M., Friction stir welding–recent developments, Material Science Forum, 426–432 (2003) 229–36.

[29] Thomas W.M., Staines D.G., Johnsonand K.I., Evans P., Com-stir–compound motion for friction stir welding and machining, Advanced Engineering Material, 5 (2003) 273–4.

[30] Buffaa G., Campanileb G., Fratini L., Priscob A., Friction stir welding of lap joints: Influence of process parameters on the metallurgical and mechanical properties, Materials Science and Engineering A, 519 (2009) 19–26.

[31] Leonard A.J., Microstructure and aging behaviour of FSW in Al alloys 2014A-T651 and 7075-T651. 2nd International Symposium on FSW (CD ROM). Gothenburg, Sweden, Composites Science and Technology, 65 (2005) 2526–40.

[32] Shamsipur Ali, Kashani-Bozorg Seyed Farshid, Zarei-Hanzaki Abbas, The effects of friction-stir process parameters on the fabrication of Ti/SiC nano-composite surface layer, Surface & Coatings Technology, 206 (2011) 1372–81.

[33] Rosso M., Mater J., Ceramic and metal matrix composites: routes and properties, Processing Technologies, 175 (2006) 364–375.

[34] Dinaharan I., Murugan N., Effect of friction stir welding on microstructure, mechanical and wear properties of AA6061/ZrB2 in situ cast composites, Materials Science and Engineering A, 543 (2012) 257–66.

[35] Ni D.R., Chen D.L., Xiao B.L., Wang D., Ma Z.Y., Residual stresses and high cycle fatigue properties of friction stir welded SiCp/AA2009 composites, International Journal of Fatigue 55 (2013) 64–73.

[36] Kumar B. Ashok, Murugan N., Optimization of friction stir welding process parameters to maximize tensile strength of stir cast AA6061-T6/AlNp composite, Materials and Design 57 (2014) 383–93.

[37] Minak G., Ceschini L., Boromei I., Ponte M., Fatigue properties of friction stir welded particulate reinforced aluminium matrix composites, International Journal of Fatigue, 32 (2010) 218–26.

[38] Uzun Huseyin, Friction stir welding of SiC particulate reinforced AA2124 aluminium alloy matrix composite, Materials and Design 28 (2007) 1440–46.

[39] Yigezu Belete Sirahbizu, Venkateswarlu D., Mahapatra M.M., Jha P.K., Mandal N.R., Technical Report On friction stir butt welding of Al + 12Si/10 wt%TiC in situ composite, Materials and Design, 54 (2014) 1019–27.

[40] Kalaiselvan K., Dinaharan I., Murugan N., Characterization of friction stir welded boron carbide particulate reinforced AA6061 aluminum alloy stir cast composite, Materials and Design, 55 (2014) 176–182.

[41] Wan Long, Huang Yongxian, Zongliang Lv, Shixiong Lv, Jicai Feng, Effect of self-support friction stir welding on microstructure and microhardness of 6082-T6 aluminum alloy joint, Materials and Design, 55 (2014) 197–203.

[42] Byung-Wook AHN, Don-Hyun CHOI, Yong-Hwan KIM, Seung-Boo JUNG, Fabrication of SiCp/AA5083 composite via friction stir welding, Transactions of Nonferrous Metals Society of China, 22 (2012) 634−638.

[43] Kumar Anand, Mahapatra M.M., Jha P.K., Mandal N.R., Devuri Venkateswarlu, Technical Report Influence of tool geometries and process variables on friction stir butt welding of Al–4.5%Cu/TiC in situ metal matrix composites, Materials and Design, 59 (2014) 406–14.

[44] Guoa J., Amira S., Gougeon P., Chen X.G., Effect of the surface preparation techniques on the EBSD analysis of a friction stir welded AA1100-B_4C metal matrix composite, Materials characterization, 62 (2011) 865 – 877.

[45] Yong-Jai Kwon, Seong-Beom Shim, Dong-Hwan Park, Friction stir welding of 5052 aluminum alloy plates, Transactions of Nonferrous Metals Society of China,19 (2009) 23−27.

[46] Cao G., Kou S., friction stir welding of 2219 aluminum: behavior of theta (Al_2Cu) particles, The Welding Journal, January 2005.

[47] Adamowski J., Gambaro C., Lertora E., Ponte M., Szkodo M., Analysis of FSW welds made of Aluminium alloy AW 6082-T6, Archives of Materials Science and Engineering, 28 (8) (2007) 453-60.

[48] Liu H.J., Fujii H., Nogi K., Friction stir welding characteristics of 2017-T351 aluminum alloy sheet, Journal of materials science, 40 (2005) 3297–99.

[49] Vural M., Ogur A., Cam G., Ozarpa C., On the friction stir welding of Aluminium alloys EN AW 2024-0 and EN AW 5754-H22, Archives of Materials Science and Engineering, 28 (2007) 49-54.

[50] Nandan R., Deb Roy T., Bhadeshia H.K.D.H, Recent Advances in Friction Stir Welding – Process, Weldment Structure and Properties, Progress in Materials Science, 53 (2008) 980-1023.

[51] Rodrigues D. M., Leitao C., Louro R., Gouveia H., Loureiro A., High speed friction stir welding of Aluminium alloys, Science and Technology of Welding and Joining, 15 (2010) 676-81.

[52] Yazdanian S., Chen Z. W., Effect of friction stir lap welding conditions on joint strength of Aluminium alloy 6060,Processing, Microstructure and Performance of materials, IOP Conference series: Material Science and Engineering, 4(2009).

[53] Merzoug Mohamed, Mazari Mohamed, Berrahal Lahcene, Imad Abdellatif, Parametric studies of the process of friction spot stir welding of Aluminium 6060-T5 alloys, Materials and Design , 31 (2010) 3023–3028.

[54] Arul S.G., Miller S.F., Kruger G.H., Pan T.Y., Mallick P.K., Shih A.J., Experimental study of joint performance in spot friction welding of 6111-T4 Aluminium alloy, Science and Technology of Welding and Joining, 13 (7) (2008) 629-37.

[55] Muruganandam D., Sreenivasan K.S., Kumar S.Ravi, Das Sushilal, Rao V.Seshagiri, Study of process parameters in friction stir welding of dissimilar Aluminium alloys, International Conference on Industrial Engineering and Operations Management Kuala Lumpur, Malaysia, (2011) 22 – 24.

[56] Sathiya P., Aravindan S., Haq A. Noorul, Optimization of friction welding parameters using evolutionary computational techniques, Journal of Materials Processing Technology, 209 (2009) 2576–84.

[57] Alves Eder Paduan, Neto Francisco Piorino, An Chen Ying, Welding of AA1050 aluminum with AISI 304 stainless steel by rotary friction welding process, Journal of Aerospace Technology and Management, 2 (2010) 301-306.

[58] Kumaran S. Senthil, Muthukumaran S., Vinodh S., Optimization of friction welding of tube to tube plate using an external tool, Structural and Multidisciplinary Optimization 42 (3) (2010) 449-457.

[59] Lakshminarayanan A. K., Balasubramanian V., Comparison of RSM with ANN in predicting tensile strength of friction stir welded AA7039 aluminium alloy joints, Transactions of Nonferrous Metals Society of China, 19 (2009) 9-18.

[60] Ericsson M., Sandstrom R., Influence of welding speed on the fatigue of friction stir welds, and comparison with MIG and TIG, International Journal of Fatigue, 25 (2003) 1379–87.

[61] Cavaliere P., Santis A. De, Panella F., Squillace A., Thermoelasticity and CCD analysis of crack propagation in AA6082 friction stir welded joints, International Journal of Fatigue, 31 (2009) 385–92.

[62] Costa J.D., Ferreira J.A.M., Borrego L.P., Abreu L.P., Fatigue behaviour of AA6082 friction stir welds under variable loadings, International Journal of Fatigue, 37 (2012) 8–16.

[63] Moreira P.M.G.P., A.M.P. de Jesus, Ribeiro A.S., P.M.S.T. de Castro, Fatigue crack growth in friction stir welds of 6082-T6 and 6061-T6 aluminium alloys: A comparison, Theoretical and Applied Fracture Mechanics, 50 (2008) 81–91.

[64] Elangovan K, Balasubramanian V. Influences of tool pin profile and welding speed on the formation of friction stir processing zone in AA2219 aluminium alloy, Journal of Materials Processing Technology, 20 (2008) 163–75.

[65] Vijay S.J., Murugan N., Influence of tool pin profile on the metallurgical and mechanical properties of friction stir welded Al–10 wt% TiB_2 metal matrix composite. Materials & Design, 31(7) (2010) 3585–9.

[66] Balasubramanian M., Jayabalan V., Balasubramanian V., A mathematical model to predict impact toughness of pulsed current gas tungsten arc welded titanium alloy. Journal of Advanced Manufacturing Technology, 35(9/10) (2008) 852-58.

[67] Kumar S., Kumar P., Shan S. H., Effect of evaporative casting process parameters on the surface roughness of Al-7%Si alloy casting, Material Processing Technology, 182 (2007) 615-23.

[68] El-Rayes M.M., El-Danaf E.A., The influence of multi-pass friction stir processingon the microstructural and mechanical properties of Aluminum Alloy 6082, Journal of Materials Processing Technology, 212 (2012) 1157–68.

[69] Dadbakhsh S., Karimi Taheri A., Smith C.W., Strengthening study on 6082 Al alloy after combination of aging treatment and ECAP process. Materials Science and Engineering, A 527 (2010) 4758–66.

[70] Zhang Z., Chen D.L., Contribution of Orowan strengthening effect in particulate reinforced metal matrix nanocomposites, Materials Science and Engineering A, 483–484 (2008) 148–152.

[71] Amirizad M., Kokabi A.H., Abbasi Gharacheh M., Sarrafi R., Shalchi B., Azizieh M. Evaluation of microstructure and mechanical properties in friction stir welded A356 + 15% SiCp cast composite. Materials Letters, 60(4) 2006 565–8.

[72] Chen X.G., Silva M. Da, Gougeon P., St-Georges L., Materials Science and Engineering A, 518 (2009) 174–184.

[73] Leitão C., Louro R., Rodrigues D.M., Analysis of high temperature plastic behaviour and its relation with weldability in friction stir welding for aluminium alloys AA5083-H111 and AA6082-T6, Materials and Design, 37 (2012) 402–9.

[74] Mroczka K., Pietras A., FSW characterization of 6082 aluminium alloys sheets Archives of Materials Science and Engineering, 40/2 (2009) 104-109.

[75] Thangarasua A., Murugan N., Dinaharan I., Production and wear characterization of AA6082 -TiC surface composites by friction stir processing, Procedia Engineering, 97 (2014) 590 – 597.

[76] Thangarasua A., Murugan N., Dinaharan I., Vijay S.J., Influnce of Traverse speed on microstructure and mechanical properties of AA6082-TiC surface composite fabricated by friction stir processing, Procedia Materials science, 5 (2014) 2115-21.

[77] Thangarasua A., Murugan N., Dinaharan I., Vijay S.J., Synthesis and characterization of titanium carbide particulate reinforced AA6082 aluminium alloy composites via friction stir processing, archives of civil and mechanical engineering, 15 (2015) 324–3 4.